Acoustic anomaly and the Landau free energy of incommensurate K_2SeO_4

Gen Li, N. Tao, Le Van Hong,* and H. Z. Cummins
Department of Physics, City College of the City University of New York, New York, New York 10031

C. Dreyfus, M. Hebbache, R. M. Pick, and J. Vagner
Departement de Recherches Physiques (URA 0071), Universite Pierre et Marie Curie, 4 place Jussieu, 75230 Paris CEDEX 05, France

(Received 26 March 1990)

Brillouin-scattering studies of the longitudinal-acoustic mode propagating along the $\mathbf{c}^*$ axis of K_2SeO_4 were performed in the vicinity of the incommensurate phase transition in both 90° and 180° scattering geometries. A theoretical derivation of the complex elastic constant $\tilde{C}_{33}(\omega)$ was carried out within the mean-field approximation including both bilinear (Landau-Khalatnikov) coupling to the amplitude mode, and anharmonic fluctuation contributions from the Σ_2 soft mode above T_I and from pairs of amplitude modes and phase modes below T_I. Comparison between theory and the Brillouin data led to an excellent fit using free-energy parameters close to values deduced from previous static and dynamical experiments. Our measurements also indicate that the phason gap $\Omega_\phi(0)$ is at least 100 GHz.

I. INTRODUCTION

Potassium selenate, K_2SeO_4, is among the most thoroughly studied crystals exhibiting structurally incommensurate phases; nevertheless a complete microscopic picture of its phase-transition sequence has not yet been established.[1] Most experiments have been analyzed on the basis of Landau-free-energy expansions with the coefficients adjusted to fit the particular experimental results. An important exception is a paper by Sannikov and Golovko who undertook a systematic evaluation of some of these coefficients in a self-consistent analysis of the results of several different experiments.[2]

K_2SeO_4 is an orthorhombic pseudohexagonal crystal with space group $D_{2h}^{16}=Pnam$ from 745 K to the incommensurate transition at $T_I=127.5$ K. Between T_I and the lock-in transition at $T_L=93$ K, it is structurally modulated with a modulation wave vector $\mathbf{q}_0=(1-\delta)\mathbf{a}^*/3$; δ decreases continuously from ~ 0.07 at T_I to ~ 0.02 at T_L, where it drops discontinuously to zero. Below T_L, K_2SeO_4 is orthorhombic with space group $C_{2v}^9=Pna2_1$ and is an improper ferroelectric with spontaneous polarization P_z. A crucial neutron-scattering study by Iizumi *et al.*[3] established that the intermediate phase is incommensurate and showed that there is a soft optic mode with wave vector $\mathbf{q}_0$ on a Σ_2 branch whose frequency approaches zero as $T\rightarrow T_I^+$, showing that K_2SeO_4 is a soft-mode driven displacive transition material.

Acoustic anomalies in K_2SeO_4 in the vicinity of the incommensurate (T_I) and lock-in (T_L) transitions have been studied by many groups with ultrasonic,[4–7] acoustic resonance,[8] and Brillouin-scattering methods.[5,9–14] An excellent overview of these effects can be found in the paper by Rehwald *et al.*,[5] who performed both ultrasonic and Brillouin-scattering experiments. The longitudinal constants C_{11} and C_{22} show only weak anomalies at T_I, while C_{33} shows a large downward step ($\sim 25\%$) with rounding both above and below the transition. Of the three longitudinal elastic constants, none show anomalies at T_L. Of the shear constants, C_{55} shows a major anomaly near T_L due to phason coupling, and C_{44} decreases continuously as T_I is approached from either side. To date, however, there has been no attempt to establish whether or not the details of the acoustic anomalies observed in these experiments can be successfully explained by the Landau free energy with coefficients determined by independent experimental data rather than being considered as free fitting parameters. Furthermore, the two principal components of the anomaly in the longitudinal elastic constants, the Landau-Khalatnikov bilinear-coupling effect and fluctuation effects, arise from the same anharmonic coupling terms in the free energy and should therefore be treated on an equal basis, which has not been done in previous studies.

We have therefore undertaken a new Brillouin-scattering study of the anomaly of the C_{33} LA mode that we will analyze with most of the free-energy coefficients fixed, in the spirit of the Sannikov-Golovko approach.[2] For this purpose, we have carried out a new theoretical analysis of the elastic constant $\tilde{C}_{33}(\omega)$ in which all anharmonic terms resulting from third-order coupling between the LA phonon and pairs of excitations lying on the soft-mode branch are taken into account simultaneously. As we will show, this analysis leads to excellent agreement with our experimental data within the framework of a self-consistent mean-field treatment of the free energy. Because the damping of longitudinal-acoustic phonons is strongly affected by coupling to pairs of phasons in the incommensurate phase, the theoretical prediction is very sensitive to the size of the $\mathbf{q}=\mathbf{0}$ gap in the phason dispersion curve. A minimum gap value of $\Omega_\phi(0)=100$ GHz is required to produce a satisfactory fit.

This paper is organized as follows. In Sec. II, we review the form of the free energy used in our analysis. In Sec. III, we summarize the results of our third-order anharmonic treatment of $\tilde{C}_{33}(\omega)$ for which the details appear in Appendix B. In Sec. IV, we explain how numerical estimates of the coefficients appearing in the theory can be obtained from available experimental data. In Sec. V, we describe the Brillouin-scattering experiments by which the temperature-dependent complex elastic constant $\tilde{C}_{33}(\omega)$ was determined at the City College of the City University of New York (CCNY) and at the Universite P.&M. Curie in Paris. In Sec. VI, we present a comparison of experiment with theory, and describe the optimization procedure leading to best-fit numerical values for the free-energy coefficients that are close to those found in Sec. IV. In Sec. VII, we compare our results with previous studies of $\tilde{C}_{33}(\omega)$ and discuss the major differences in the theoretical analysis underlying the improved agreement obtained in this study. Finally, in Sec. VIII, we summarize the principal results of our study. We also briefly discuss the question of a theoretical approach going beyond the mean-field approximation. Such a theory should be based on the three-dimensional (3D) XY model, which is the appropriate universality class for a two-component order-parameter system like K_2SeO_4, and for which a number of results are already available.

II. THE LANDAU FREE ENERGY

The Landau free energy for incommensurate crystals is most frequently written as a functional $f(x)$ in which the order parameter $Q(x)$ is the complex position-dependent amplitude of the Σ_2 soft mode at the commensurate wave vector $\mathbf{q}_c$. This form has the great advantage of describing both the incommensurate and lock-in transitions, as well as the evolution of the modulation wave from the sinusoidal regime near T_I to the multisoliton regime near T_L,[15] but does not naturally include dynamics. In Appendix A, we show how this form of the free-energy density $F=(1/v)\int f(x)\,dv$ can be approximated, in the temperature range above and just below the incommensurate transition temperature T_I, by

$$F=\tfrac{1}{2}A_0(T-T_I)\rho^2+\tfrac{1}{4}B\rho^4+\tfrac{1}{6}D\rho^6+\tfrac{1}{2}\sum_{i,j=1}^{3}C_{ij}\epsilon_i\epsilon_j - \sum_{i=1}^{3}h_i\epsilon_i\rho^2+\sum_{i=1}^{3}g_i\epsilon_i^2\rho^2 , \tag{2.1}$$

where ρ is the amplitude of the Σ_2 soft mode that will condense, below T_I, producing a static modulation with the incommensurate wave vector $\mathbf{q}_0$, ϵ_i are the strains, and the continuum constant amplitude approximation has been employed.

Although this form of the free energy can be extended to analyze the interactions of acoustic phonons with the order-parameter dynamics,[16] it is more consistent for dynamical analysis in the vicinity of T_I to proceed from a free-energy density written directly as an expansion in normal-mode coordinates. We shall use such an expansion in our analysis, although this form of F cannot be extended easily to the multiple-soliton regime near the lock-in transition, where higher-order harmonics become increasingly important.

The relevant part of the free-energy density, expressed directly in normal-mode coordinates, can be written as

$$F=F_1+F_{\text{el}}+F_c , \tag{2.2}$$

F_1 is the part of the free energy that depends only on the normal coordinates $Q(\mathbf{q})$ on the branch where the modes at $\mathbf{q}_0$ (and $-\mathbf{q}_0$) become critical at T_I; F_{el} is the purely elastic contribution, which will be expressed either in terms of the elastic strain, ϵ_i or in terms of the corresponding acoustic phonon coordinates, $iq_\alpha U_\beta/\sqrt{\rho_m}$, where α and β are Cartesian indices, $\mathbf{q}$ is a wave vector, $\mathbf{U}/\sqrt{\rho_m}$ is the corresponding displacement, and ρ_m is the mass density; F_c is the coupling term between the $Q(\mathbf{q})$ and the ϵ_i, of which we will take into account only the lowest-order contributions.

For the present problem, F_1 is given by

$$\begin{aligned}F_1=&\sum_{\mathbf{q}_1,\mathbf{q}_2}\tfrac{1}{2}\Omega^2(\mathbf{q}_1)Q(\mathbf{q}_1)Q(\mathbf{q}_2)\delta(\mathbf{q}_1+\mathbf{q}_2)\\ &+\sum_{\mathbf{q}_1,\ldots,\mathbf{q}_4}\tfrac{1}{6}BQ(\mathbf{q}_1)\cdots Q(\mathbf{q}_4)\delta(\mathbf{q}_1+\mathbf{q}_2+\mathbf{q}_3+\mathbf{q}_4)\\ &+\sum_{\mathbf{q}_1,\ldots,\mathbf{q}_6}\tfrac{1}{15}DQ(\mathbf{q}_1)\cdots Q(\mathbf{q}_6)\delta(\mathbf{q}_1+\mathbf{q}_2\cdots+\mathbf{q}_6) .\end{aligned} \tag{2.3}$$

In this expression, it is understood that $Q(\mathbf{q})$, the normal coordinate of a mode on the soft branch, is considered only for $\mathbf{q}$ in the vicinity of $\mathbf{q}_0$ or $-\mathbf{q}_0$. Furthermore, we have neglected the wave-vector variation of both the B and D coefficients, while the $\mathbf{q}$ dependence of Ω is included as

$$\Omega^2(\mathbf{q})=A_0(T-T_I)+\tfrac{1}{2}\sum_{\alpha,\beta}\Lambda_{\alpha\beta}(\mathbf{q}\mp\mathbf{q}_0)_\alpha(\mathbf{q}\mp\mathbf{q}_0)_\beta , \tag{2.4}$$

the $\mp$ sign depending on the proximity of $\mathbf{q}$ to $+\mathbf{q}_0$ or $-\mathbf{q}_0$, and $\Lambda_{\alpha\beta}$ being a symmetric tensor with the full orthorhombic symmetry. F_{el} is the usual elastic energy [given by the fourth term on the right-hand side (rhs) of Eq. (2.1)], while the coupling term between the principal strains $(i,j=1,2,3)$ and the relevant phonons is

$$F_c=\sum_{i=1}^{3}\sum_{\mathbf{q}_1,\mathbf{q}_2}(h_i\epsilon_i-g_i\epsilon_i^2)Q(\mathbf{q}_1)Q(\mathbf{q}_2)\delta(\mathbf{q}_1+\mathbf{q}_2) . \tag{2.5}$$

The above free energy is written in the variables relevant to $T>T_I$. A complete treatment of Eq. (2.2) and the corresponding exact behavior of the elastic constant is impossible to obtain. Therefore, in the present study, we shall neglect the role of D [Eq. (2.3)] and g [Eq. (2.5)] except for the modifications they produce in the static properties of the incommensurate phase. Furthermore, the term proportional to B [Eq. (2.3)] will be used for stabilizing the incommensurate phase and modifying the dynamics of the corresponding mode, but its influence on the anharmonic properties of the crystal will be neglected.

The free energy of Eqs. (2.2)–(2.5) contains both equilibrium and dynamical components. The equilibrium components can be obtained by dropping all terms in the sums except those for which all $\mathbf{q}_i$ are equal to $\mp\mathbf{q}_0$ and setting $Q(\mathbf{q}_0)=(1/\sqrt{2})\rho e^{i\phi}$, from which (neglecting all strains except ϵ_1, ϵ_2, and ϵ_3) one obtains

$$F_{\rm eq}=\tfrac{1}{2}\Omega^2(\mathbf{q}_0)\rho^2+\tfrac{1}{4}B\rho^4+\tfrac{1}{6}D\rho^6 +\tfrac{1}{2}\sum_{i,j=0}^{3} C_{ij}\epsilon_i\epsilon_j-\sum_{i=1}^{3}(h_i\epsilon_i-g_i\epsilon_i^2)\rho^2 \ . \qquad (2.6)$$

Comparison of Eq. (2.6) with Eq. (2.1) shows that the two expressions for $F_{\rm eq}$ are identical, since $\Omega^2(\mathbf{q}_0)=A_0(T-T_I)$, as shown in Eq. (2.4).

III. DERIVATION OF THE ELASTIC ANOMALY

The three longitudinal strains ϵ_1, ϵ_2, and ϵ_3 are coupled to the order parameter ρ through the term $(h_i\epsilon_i-g_i\epsilon_i^2)Q(\mathbf{q})Q^*(\mathbf{q})$ in our free-energy expansion [Eq. (2.5)]. Experimentally, however, only the ϵ_3 LA mode shows a major anomaly near T_I, a rounded step in $C'_{33}(\omega)$, whose value decreases by approximately 25% in the immediate vicinity of the transition.[5]

Such an effect is not unusual: it has been found in many other structural transitions in which bilinear coupling of strains to the order parameter is forbidden by symmetry, and is often associated with improper ferroelasticity. Nevertheless, even within the simplified framework of a mean-field theory, a complete treatment of the effect has never been given in the case of a normal-incommensurate phase transition, and the acoustic-phonon–phason coupling has never been completely analyzed. Therefore, in this section, we shall first briefly review the salient features of the acoustic anomaly for the case of an ordinary second-order commensurate-commensurate phase transition, and then sketch the new aspects for a commensurate-incommensurate transition. The details of the calculation are given in Appendix B.

For an ordinary phase transition, with the same free energy [Eqs. (2.2)–(2.5)], the acoustic anomaly has two origins that can be summarized as follows. Neglecting, for clarity, the g term in Eq. (2.5), concentrating on ϵ_3, and considering a zone-center transition ($\mathbf{q}_0=\mathbf{0}$), Eq. (2.5) can be reduced to

$$F_c=h_3\epsilon_3\left[Q^2(0)+\sum_{\mathbf{q}}{}' Q(\mathbf{q})Q^*(\mathbf{q})\right] \ . \qquad (3.1)$$

One of the two origins of the acoustic anomaly is that, below the transition temperature T_0, (a) $\langle Q(0)\rangle=\rho_0$ is different from zero, and close to T_0, proportional to $(T_0-T)^{1/2}$, while ϵ_3^0 is proportional to ρ_0^2. (b) The soft mode frequency $\Omega(0)$ is renormalized, due to the nonzero values of ρ_0 and ϵ_3^0, and also becomes proportional to $(T_0-T)^{1/2}$ in the vicinity of T_0.

Replacing one of the two normal-mode coordinates $Q(0)$ in Eq. (3.1) by its thermal mean value ρ_0, the first term in Eq. (3.1) yields a linear coupling proportional to the order parameter between the elastic strain and the soft mode. Furthermore, due to ordinary anharmonic interactions between this soft mode and all other phonon branches, this soft mode has a linewidth Γ, which can be assumed to be wave-vector independent in the vicinity of $\mathbf{q}_0=\mathbf{0}$, and is also noncritical at T_0. Its value is proportional to T if third-order anharmonicity is predominant. The frequency-dependent elastic constant can then be written, including this coupling to a damped oscillator, as

$$C_{33}(\omega)=C_{33}^0-\frac{4h_3^2\rho_0^2(T)}{\Omega^2(T)-i\omega\Gamma-\omega^2} \ , \qquad (3.2)$$

where $\Omega(T)$ is the temperature-dependent soft-mode frequency $\Omega(0)$.

In the static limit $\omega=0$ this leads to the usual jump of C_{33} at T_0 [see Eq. (4.10) below]. At Brillouin frequencies, if the soft mode is overdamped ($\omega<\Omega<\Gamma$), one obtains the classical Landau-Khalatnikov result[17]

$$C_{33}(\omega)=C_{33}^0-\frac{4h_3^2\rho_0^2(T)}{\Omega^2(T)}\frac{1}{1-i\omega\dfrac{\Gamma}{\Omega^2(T)}} \ , \qquad (3.3)$$

which shows that the experimental result is indistinguishable from a coupling of ϵ_3 to a simple Debye relaxational mode of relaxation time $\tau=[\Gamma/\Omega^2(T)]$, with τ diverging at T_0. Well below T_0, $\omega\tau\rightarrow 0$, and the static result is recovered. Note that Eq. (3.3) does not lead to any effect above T_0, contrary to experimental evidence, indicating the presence of a second effect.

The origin of this second effect is the second term in Eq. (3.1). Above T_0, as $\Omega(T)$ tends to zero, the amplitude of the phonons on the soft branch close to $\mathbf{q}_0=\mathbf{0}$ increases enormously, giving a rapid increase in the weight of this anharmonic term summed over all wave vectors of this branch in the vicinity of the Brillouin-zone center. As shown by Levanyuk et al.,[18] this second contribution, which depends on the same coefficient h_3, is given by

$$\Delta C_{33}(\omega)=-(k_BT)\frac{2h_3^2}{(2\pi)^3}\int\frac{d^3q}{\Omega^2(\mathbf{q})\left[\Omega^2(\mathbf{q})-i\omega\dfrac{\Gamma}{2}\right]} \ , \qquad (3.4)$$

involving the soft-mode dispersion curve and damping constant. Note that in Eq. (3.4), the main contribution to the integral (often designated as the fluctuation integral) comes from the vicinity of $\mathbf{q}_0=\mathbf{0}$, where $\Omega(\mathbf{q})$ is a minimum.[19–21] Equation (3.4) is also valid below the phase transition, where the frequency of all the phonons of the soft branch are renormalized by the nonzero values of ρ_0 and ϵ_3^0. Equations (3.2) and (3.4) thus describe the two effects that produce the elastic anomalies in the vicinity of T_0 for an ordinary phase transition.

The situation in the vicinity of a commensurate-incommensurate phase transition at T_I is more complex. First, since $\mathbf{q}_0\neq\mathbf{0}$, the star of $\mathbf{q}_0$ consists of at least two distinct wave vectors, $\mathbf{q}_0$ and $-\mathbf{q}_0$ (the case to which we shall restrict ourselves), involving two soft modes (and two critical regions in the soft phonon branch) above T_I. Below T_I these two soft modes give rise to two other excitations, the amplitudon (which is the usual soft mode) and the phason which, to lowest order in $(T_I - T)$, has a temperature-independent dispersion curve that is linear in $\mathbf{K}=\mathbf{q}-\mathbf{q}_0$.

The phase mode, with its $|\mathbf{K}|$-linear dispersion, is of odd parity like an acoustic phonon, but has the same damping as the soft mode above T_I or the amplitude mode below T_I, and is thus always overdamped for small $\mathbf{K}$.

The influence of the phason on the Landau-Khalatnikov term has been frequently considered.[22-25] Since an acoustic strain has even parity while the phase mode has odd parity, the corresponding phase-mode-coupling coefficient, h_3^ϕ, is equal to zero for $\mathbf{K}=\mathbf{0}$. When considered as a function of $\mathbf{K}$, it can be written as $h_3^\phi(\mathbf{K})$ and expanded in powers of $\mathbf{K}$. For the present case, the term corresponding to Eq. (3.2) now adds a contribution:

$$-4[h_3^\phi(\mathbf{K})]^2 \frac{\rho_0^2(T)}{\Omega_\phi^2(\mathbf{K}) - i\omega\Gamma - \omega^2} \tag{3.5}$$

with, to first order in $\mathbf{K}$,

$$\Omega_\phi(\mathbf{K}) = V(\mathbf{K}/|\mathbf{K}|)|\mathbf{K}| , \tag{3.6}$$

$$h_3^\phi(\mathbf{K}) = \sum_{i=1}^{3} h_{3i}^\phi K_i . \tag{3.7}$$

In the $\omega \to 0$ limit, Eq. (3.5) has a nonzero value for $|\mathbf{K}| \to 0$ with the direction of $\mathbf{K}$ fixed, and adds to the static elastic constant a term that is different from the Landau-Khalatnikov contribution discussed in Eq. (3.2). While the corresponding term is allowed for a LA phonon propagating along $\mathbf{a}^*$ and gives a contribution to C_{11}, in the present case where $\mathbf{K}=K_3\mathbf{c}^*$, the coefficient h_{33}^ϕ is equal to zero by symmetry, and we can ignore Eq. (3.5) in the case of C_{33}.

The anharmonic contribution, which led to Eq. (3.4), cannot be ignored. Below T_I, coupling to both the amplitudon and the phason must be considered; the longitudinal strain can be coupled to two amplitudons, to one amplitudon and one phason, or to two phasons. The first case (two amplitudons) is identical to the coupling to the two soft modes given in Eq. (3.4).

The second case involves the coupling of an even variable ϵ_3 to the product of an even variable (amplitudon) and an odd variable (phason). This coupling, as in the case discussed before Eq. (3.5), is equal to zero for $\mathbf{K}=0$, and has to be developed in successive powers of $\mathbf{K}$ [cf. Eq. (3.7)]. In K_2SeO_4, only h_{31}^ϕ is different from zero; nevertheless, in the summation over $\mathbf{K}$, i.e., in the vicinity of $\mathbf{q}_0$, the most important contribution comes from the points where both the amplitudon and the phason have a small frequency, i.e, for small $|\mathbf{K}|$. As the coupling term corresponding to h_3^2 in Eq. (3.4) would be $(h_{31}^\phi K_1)^2$, which is quadratic in the wave vector, we shall neglect this anharmonic contribution.

The situation is different for the third case (anharmonic coupling between ϵ_3 and two phasons). The product of two phason coordinates is even, and the calculation shows that the coupling coefficient is the same as for the case of two amplitudons. This contribution has thus to be considered on the same basis as that due to the amplitudons. Furthermore, as the phason frequencies do not vary with temperature, this term can play a much more important role than the amplitudon contribution a few degrees below T_I. It has thus been introduced, for the first time, in our present study of the acoustic anomaly of $\tilde{C}_{33}(\omega)$.

The details of the relevant calculations are given in Appendix B, where the complete free-energy form of Eqs. (2.2)–(2.5) was used. The detailed expressions for the complex elastic constant $\tilde{C}_{33}(\omega)$ are given in Eqs. (B18) and (B19). For the analysis of Brillouin-scattering data, we will use the Brillouin shift $\Delta\omega_B = q_3[C'_{33}(\omega)/\rho_m]^{1/2}$ and linewidth (full width at half maximum) (FWHM) $\gamma_{33}(\omega) = (q_3^2/\rho_m)[C''_{33}(\omega)/\omega]$ (which are also the frequency and damping constant of the acoustic phonon with wave vector $q_3\mathbf{c}^*/|\mathbf{c}^*|$), where ρ_m is the mass density. We give here the expressions for $C'_{33}(\omega)$ and $\gamma_{33}(\omega)$. After adding a "background" acoustic-mode damping γ_{33}^0 and assuming that $\omega^2 \ll \Omega_A^2(0)$, the theoretical predictions for the temperature dependence of $C'_{33}(\omega)$ and $\gamma_{33}(\omega)$ found from Eqs. (B18) and (B19) are

$T > T_I$:

$$C'_{33}(\omega) = C_{33}^0 - \frac{16k_B T}{(2\pi)^3} h_3^2 \int \frac{d\mathbf{K}}{4\Omega_2^4(\mathbf{K}) + \omega^2\Gamma_2^2(\mathbf{K})} , \tag{3.8}$$

$$\gamma_{33}(\omega) = \gamma_{33}^0 + \frac{8q_3^2}{\rho_m} \frac{k_B T}{(2\pi)^3} h_3^2 \int \frac{\Gamma_2(\mathbf{K}) d\mathbf{K}}{\Omega_2^2(\mathbf{K})[4\Omega_2^4(\mathbf{K}) + \omega^2\Gamma_2^2(\mathbf{K})]} , \tag{3.9}$$

$T < T_I$:

$$\begin{aligned} C'_{33}(\omega) = {} & (C_{33}^0 + 2g_3\rho_0^2) - \frac{4(h_3 - 2g_3\epsilon_3^0)^2 \rho_0^2 \Omega_A^2(0)}{\Omega_A^4(0) + \omega^2\Gamma_A^2(0)} \\ & - \frac{8k_B T}{(2\pi)^3}(h_3 - 2g_3\epsilon_3^0)^2 \left[\int \frac{d\mathbf{K}}{4\Omega_A^4(\mathbf{K}) + \omega^2\Gamma_A^2(\mathbf{K})} + \int \frac{d\mathbf{K}}{4\Omega_\phi^4(\mathbf{K}) + \omega^2\Gamma_\phi^2(\mathbf{K})} \right] \end{aligned} \tag{3.10}$$

$$\gamma_{33}(\omega)=\gamma_{33}^0+\frac{4q_3^2}{\rho_m}\frac{(h_3-2g_3\epsilon_3^0)^2\rho_0^2\Gamma_A(0)}{\Omega_A^4(0)+\omega^2\Gamma_A^2(0)}$$
$$+\frac{4q_3^2}{\rho_m}\frac{k_BT}{(2\pi)^3}(h_3-2g_3\epsilon_3^0)^2\left[\int\frac{\Gamma_A(\mathbf{K})d\mathbf{K}}{\Omega_A^2(\mathbf{K})[4\Omega_A^4(\mathbf{K})+\omega^2\Gamma_A^2(\mathbf{K})]}+\int\frac{\Gamma_\phi(\mathbf{K})d\mathbf{K}}{\Omega_\phi^2(\mathbf{K})[4\Omega_\phi^4(\mathbf{K})+\omega^2\Gamma_\phi^2(\mathbf{K})]}\right]. \quad (3.11)$$

In Eqs. (3.8)–(3.11), Ω_2, Γ_2, Ω_A, Γ_A, Ω_ϕ, and Γ_ϕ are the frequencies and damping constants of the Σ_2 soft-mode, the amplitude-mode, and the phase-mode branches, respectively. Expressions for Ω_2, Ω_A, and Ω_ϕ are given in Eqs. (2.2), (4.14), and (4.16). For clarity, we have used different symbols for the three linewidths and indicated a wave-vector dependence, although, as mentioned previously, we shall consider them as equal and $\mathbf{K}$ independent in carrying out the analysis.

Finally, because the dispersion curves of $\Omega_A(\mathbf{K})$ and $\Omega_\phi(\mathbf{K})$ are only known in the vicinity of their minima, a definite procedure has to be defined for their evaluation. This question will be discussed in Sec. VI, after we have explained how the coefficients appearing in Eqs. (2.1) and (2.4) have been extracted from experimental data.

The predictions of Eqs. (3.8)–(3.11), using free-energy coefficients evaluated in Sec. IV, are shown in Fig. 5.

IV. FREE-ENERGY COEFFICIENTS

Many of the coefficients appearing in the full free-energy expansion [Eqs. (A1)–(A4)] can be determined from the existing experimental literature on K_2SeO_4 as discussed by Sannikov and Golovko.[2] Here, however, we will only consider the coefficients A_0, B, D, C_{ij} $(i,j=1,2,3)$, h_1, h_2, h_3, and g_3 appearing in the reduced free energy of Eq. (2.1) (ignoring all g_i except g_3) as well as the three components of the diagonal tensor $\Lambda_{\alpha\alpha}=\delta_{\alpha\beta}\Lambda_{\alpha\beta}$ in Eq. (2.4).

(1) A_0: The coefficient A_0, which is related to the soft-mode frequency above T_I by $\Omega_2^2(\mathbf{q}_0)=A_0(T-T_I)$, can be determined from the inelastic-neutron-scattering data of Iizumi *et al.*[3] Their Fig. 7 shows the squares of the Σ_2 soft-mode phonon energies at $\mathbf{q}_0=(0.31,0,0)$ from T_I to 250 K. A linear fit to these points gives $[\hbar\Omega_2(\mathbf{q}_0)]^2=0.07(T-T_I)$ $\mathrm{meV^2\,K^{-1}}$, from which $A_0=1.6\times10^{23}\ \mathrm{s^{-2}\,K^{-1}}$.

(2) C_{ij}^0: We have estimated the "bare" values of the elastic constants C_{ij}^0 by extrapolating the results of previous ultrasonic and Brillouin-scattering studies to T_I.[5,12] We find for $[C^0]$ in units of $\mathrm{dyn\,cm^{-2}}$ and $[S^0]$ in units of $\mathrm{dyn^{-1}\,cm^2}$,

$$[C^0]=\begin{bmatrix}5.8\times10^{11} & 1.7\times10^{11} & 1.5\times10^{11}\\ & 5.4\times10^{11} & 2.0\times10^{11}\\ & & 4.0\times10^{11}\end{bmatrix},$$

$$[S^0]=[C^0]^{-1}=\begin{bmatrix}0.20\times10^{-11} & -0.045\times10^{-11} & -0.045\times10^{-11}\\ & 0.23\times10^{-11} & -0.10\times10^{-11}\\ & & 0.32\times10^{-11}\end{bmatrix}.$$

(3) B and h_i: These coefficients can be evaluated from the observed jumps in the specific heat (ΔC_P) and thermal expansion coefficients $(\Delta\alpha_i)$ at T_I.

The specific heat of K_2SeO_4 has been measured by several authors.[26–30] The most recent results of Flerov *et al.*[29] are $\Delta C_P=10.1\ \mathrm{J\,K^{-1}\,mol^{-1}}$. This value, together with the molar volume of $72.1\ \mathrm{cm^3\,mol^{-1}}$ ($\rho_m=3.05\ \mathrm{g\,cm^{-3}}$, 1 mol=221 g) gives

$$\Delta C_P=1.4\times10^6\ \mathrm{erg\,cm^{-3}\,K^{-1}}.$$

The thermal expansion of K_2SeO_4 has also been studied by several authors.[29,31–33] The results of Flerov *et al.*[29] show anomalies $\Delta\alpha_1$, $\Delta\alpha_2$, $\Delta\alpha_3$ in the α_i at T_I of 3.4×10^{-5}, 8.1×10^{-5}, $-19.1\times10^{-5}\ \mathrm{K^{-1}}$, respectively.

Very close to T_I, the approximate free energy of Eq. (2.1) can be further reduced by ignoring the sixth power and biquadratic terms, giving

$$F\cong F_0+\tfrac{1}{2}A\rho^2+\tfrac{1}{4}B\rho^4+\tfrac{1}{2}\epsilon_iC_{ij}\epsilon_j-h_i\epsilon_i\rho^2, \quad (4.1)$$

where summation over repeated indices is assumed, and $1\le i,j\le3$.

The spontaneous strains at zero stress, found by minimizing F with respect to ϵ_i, are

$$\epsilon_i^0=[C^{-1}]_{ij}h_j\rho_0^2. \quad (4.2)$$

Using this result to eliminate the ϵ_i, the free energy at zero stress is

$$F(T\sim T_I,\sigma_i=0)=F_0+\tfrac{1}{2}A\rho_0^2+\tfrac{1}{4}B'\rho_0^4, \quad (4.3)$$

where

$$B'=B-2h_i[C^{-1}]_{ij}h_j. \quad (4.4)$$

The equilibrium value of the order parameter near T_I (from $\partial F/\partial\rho=0$) is $\rho_0^2=0$ $(T>T_I)$ and $\rho_0^2=-A/B'$ $(T<T_I)$ so that

$$F = F_0 \quad (T > T_I) ,$$
$$F(\epsilon_i = \epsilon_i^0, \rho = \rho_0) = F_0 - \frac{A^2}{4B'} \quad (T \lesssim T_I) . \tag{4.5}$$

The specific heat $C_P = -T(\partial^2 F/\partial T^2)_{(\epsilon_i^0, \rho_0)}$ is then

$$C_P = C_P^0 \quad (T > T_I) , \tag{4.6a}$$

$$C_P = C_P^0 + \frac{TA_0^2}{2B'} \quad (T \lesssim T_I) , \tag{4.6b}$$

where $C_P^0 = -T(\partial^2 F_0/\partial T^2)_{(\epsilon_i^0, \rho_0)}$ is the background specific heat due to other degrees of freedom. The jump in C_P at T_I is therefore

$$\Delta C_P = T_I A_0^2 / 2B' . \tag{4.7}$$

Similarly, the thermal expansion coefficients $\alpha_i = (\partial \epsilon_i^0 / \partial T)$ are, from Eq. (4.2), $\alpha_i = [C^{-1}]_{ij} h_j (\partial \rho_0^2 / \partial T)$, so that

$$\alpha_i = \alpha_i^0 \quad (T > T_I) ,$$

$$\alpha_i = \alpha_i^0 - [C^{-1}]_{ij} h_j \frac{A_0}{B'} \quad (T \lesssim T_I) ,$$

and the jump in α_i at T_I is

$$\Delta \alpha_i = \frac{-A_0}{B'} [C^{-1}]_{ij} h_j . \tag{4.8}$$

Combining Eqs. (4.7) and (4.8),

$$h_i = \frac{-A_0 T_I}{2} C_{ij} \frac{\Delta \alpha_j}{\Delta C_P} ,$$

while from Eqs. (4.4) and (4.7),

$$B = \frac{1}{2} \left[\frac{T_I A_0^2}{\Delta C_P} + 4 h_i [C^{-1}]_{ij} h_j \right] . \tag{4.9}$$

Evaluating Eqs. (4.8) and (4.9) gives

$$B = 2.1 \times 10^{42} \text{ g}^{-1} \text{cm s}^{-2} ,$$

$$[h_1, h_2, h_3] = (-0.42, \ -0.80, \ 3.8) \times 10^{26} \text{ s}^{-2} .$$

An auxiliary check of these values is supplied by the downward step in C_{33} at T_I, which experimentally is approximately 11×10^{10} dyn cm^{-2}. From Eqs. (3.8) and (3.10), the static elastic constant $\tilde{C}_{33}(0)$ of the free crystal, modified by the cubic coupling to the order parameter, is

$$\tilde{C}_{33}(0) = C_{33}^0 \quad (T > T_I) , \tag{4.10a}$$

$$\tilde{C}_{33}(0) = C_{33}^0 - \frac{4h_3^2 \rho_0^2}{\Omega_A^2(0)} = C_{33}^0 - \frac{2h_3^2}{B} \quad (T < T_I) , \tag{4.10b}$$

from which $\Delta \tilde{C}_{33}(0) = -2h_3^2/B = -14 \times 10^{10}$ dyn cm^{-2}, in reasonably good agreement with observation.

(4) D and g_3: The coefficients of the ρ^6 term and the biquadratic term in Eq. (2.1) (D and g_3) cannot be properly evaluated from existing experimental data, but their values can be estimated from the temperature dependence of the spontaneous strain ϵ_3^0 in the incommensurate phase, as determined from x-ray-diffraction data by Kudo and Ikeda.[32] The equilibrium conditions obtained from Eq. (2.1) are

$$A_0(T - T_I) + B\rho_0^2 + D\rho_0^4 - 2h_3 \epsilon_3^0 + 2g_3(\epsilon_3^0)^2 = 0 , \tag{4.11a}$$

$$\epsilon_i^0 = [C^{-1}]_{ij} (h_j - 2\delta_{j3} g_3 \epsilon_3^0) \rho_0^2 , \tag{4.11b}$$

from which $\rho_0(T)$ and $\epsilon_i^0(T)$ can, in principle, be deduced

TABLE I. Free energy coefficients.

Coefficient	Value found from previous experiments[a]	Best fit of $C'_{33}(\omega)$ and $\gamma_{33}(\omega)$ to present experiments (mean field)
A_0 ($\text{s}^{-2}\text{K}^{-1}$)	1.6×10^{23}	
B ($\text{g}^{-1}\text{cm s}^{-2}$)	2.1×10^{42}	2.1×10^{42} (with $D = 0$) 2.0×10^{42} (with $g_3 = 0$)
D ($\text{g}^{-2}\text{cm}^2\text{s}^{-2}$)	0.42×10^{60} (with $g_3 = 0$)	0.36×10^{60} (with $g_3 = 0$)
$[C^0]$ (dyn cm^{-2})	$\begin{bmatrix} 5.8\times10^{11} & 1.7\times10^{11} & 1.5\times10^{11} \\ & 5.4\times10^{11} & 2.0\times10^{11} \\ & & 4.0\times10^{11} \end{bmatrix}$	
h_1 (s^{-2})	-0.42×10^{26}	
h_2 (s^{-2})	-0.80×10^{26}	
h_3 (s^{-2})	3.8×10^{26}	3.5×10^{26}
g_3 (s^{-2})	1.8×10^{-28} (with $D = 0$)	1.2×10^{-28} (with $D = 0$)
Λ_x ($\text{THz}^2\,\text{Å}^2$)	3.2	
$\Lambda_y = \Lambda_z$ ($\text{THz}^2\,\text{Å}^2$)	17	
Γ (THz)	$0.0027(T - T_I) + 0.34$	
$\Omega_\phi(0)$ (GHz)	60 ± 25	

[a] As described in Sec. IV of the text. The values found by Sannikov and Golovko (Ref. 2) are given in Ref. 35.

if g_3 and D are known. Treating D or g_3 as a fitting parameter and fitting ϵ_3^0 to the experimental data, one can deduce the best value of either D or g_3, setting the other one equal to zero. If $D=0$, a best fit is obtained with $g_3=1.8\times10^{-28}$ s^{-2}. Conversely, if $g_3=0$, we find $D=0.42\times10^{60}$ $g^{-2}\,cm^2\,s^{-2}$.

(5) Λ_i: The dispersion of the Σ_2 soft optic branch near $\mathbf{K}=0$ can be represented by

$$\Omega_2^2(\mathbf{q})=\Omega_2^2(\mathbf{q}_0)+\tfrac{1}{2}\Lambda_x K_x^2+\tfrac{1}{2}\Lambda_y K_y^2+\tfrac{1}{2}\Lambda_z K_z^2 . \qquad (4.12)$$

From Iizumi *et al.*[3] (at 130 K), $\Lambda_x=3.2$ THz Å^2, $\Lambda_z=17$ THz^2 Å^2. Λ_y was not determined, so we assume that $\Lambda_y=\Lambda_z$. We also assume that Λ_x and Λ_z are temperature independent and have the same value above and below T_I.

(6) Γ: In agreement with Quilichini and Currat,[34] for the whole temperature range under study, we assume a $\mathbf{K}$-independent damping constant and represent its temperature variation by

$$\Gamma=[0.0027(T-T_I)+0.34]\ \text{THz} . \qquad (4.13)$$

Having evaluated all the relevant free-energy coefficients, and rewriting Eqs. (B11b) and (B11c) as

$$\Omega_A^2(\mathbf{K})=2B\rho_0^2+4D\rho_0^4+\tfrac{1}{2}\Lambda_x K_x^2+\tfrac{1}{2}\Lambda_z(K_y^2+K_z^2) , \qquad (4.14)$$

$$\Omega_\phi^2(\mathbf{K})=\tfrac{1}{2}\Lambda_x K_x^2+\tfrac{1}{2}\Lambda_z(K_y^2+K_z^2) , \qquad (4.15)$$

we are now in a position to compute $C'_{33}(\omega)$ and $\gamma_{33}(\omega)$ [Eqs. (3.8)–(3.11)] as functions of temperature.

Currat and Quilichini have verified, in their inelastic-neutron-scattering experiments on the phason dispersion, that Γ, Λ_x, and Λ_z deduced from Eq. (4.15) are consistent with the values obtained above T_I as we have assumed. However, their data indicate a nonzero phason frequency at $\mathbf{K}=0$, $\Omega_\phi(0)=(60\pm25)$ GHz, contrary to Eq. (4.15). We shall therefore add a phason-gap term, $\Omega_\phi(0)$, to this equation and rewrite it as

$$\Omega_\phi^2(\mathbf{K})=\Omega_\phi^2(0)+\tfrac{1}{2}\Lambda_x K_x^2+\tfrac{1}{2}\Lambda_z(K_y^2+K_z^2) . \qquad (4.16)$$

The values of all the coefficients evaluated in this section are given in the second column of Table I.

V. BRILLOUIN-SCATTERING EXPERIMENTS

The K_2SeO_4 crystals used in our experiments were grown by Hauret at the Universite d'Orleans from 99% stock material (Alfa Products, Danvers, Massachusetts) that was recrystallized twice for purification.

(1) New York: 90° scattering experiments were performed with a crystal approximately 6 mm on each side, cut with faces perpendicular to $\mathbf{b}$, $\mathbf{a}+\mathbf{c}$, and $\mathbf{a}-\mathbf{c}$. The scattering geometry used was $(\mathbf{a}+\mathbf{c})[\mathbf{b},T](\mathbf{a}-\mathbf{c})$. The crystal was mounted on the cold finger of a Cryotip continuous-flow nitrogen cryostat controlled by an Oxford ITC-4 platinum resistance temperature controller with accuracy $\sim\pm0.1$ K. A Spectra-Physics 165 single-mode argon-ion laser provided 100 mW of incident v-polarized light at 488 nm. Scattered light was analyzed with a six-pass (3×2) Sandercock tandem Fabry-Perot interferometer with finesse ~70. 7- or 16-mm plate separations were used, and the interferometer was scanned at 2 scans per second. A schematic illustration of the experimental apparatus is shown in Fig. 1.

Data were acquired with an AT-type computer equipped with an EG&G multiscalar board. 1024 (or 3072) data channels were stored, typically for 3 000 scans near T_I and 1 200 scans far from T_I, where the Brillouin

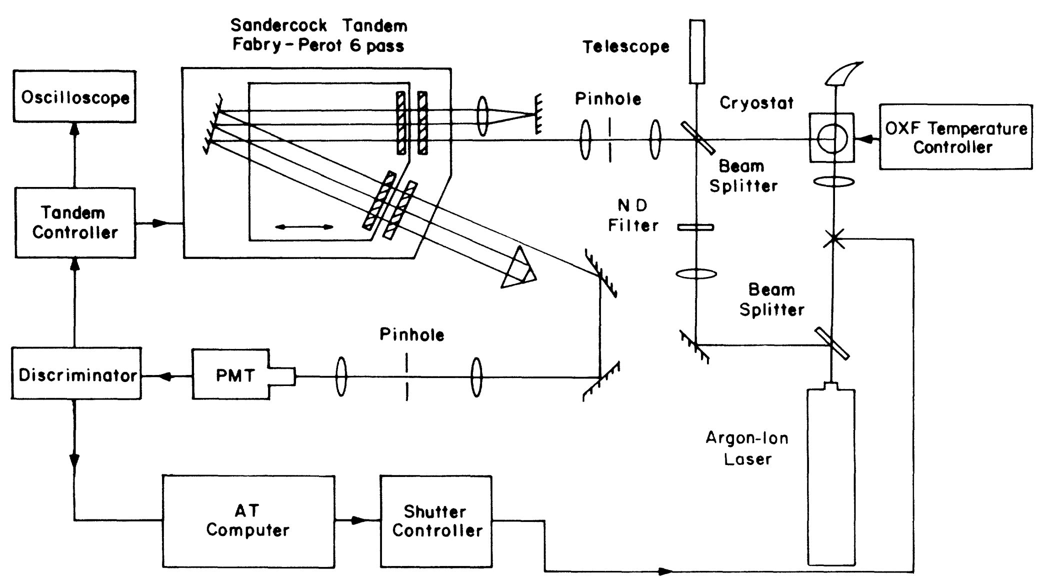

FIG. 1. Schematic illustration of the CCNY six-pass tandem interferometer Brillouin scattering apparatus. (ND denotes neutral density filter.)

lines are narrow. Data were subsequently transferred to the CCNY Science Division Vax 780 for analysis with a nonlinear least squares fitting program.

Figure 2 shows three Brillouin spectra, at $T = 300$, 127.5, and 81 K. Note the evident broadening at 127.5 K.

(2) Paris: Experiments were carried out in the backscattering 180° geometry with a crystal cut parallel to the crystallographic axes. The scattering geometry was: $c[b,T]c$. The crystal was mounted in a homemade cryostat with helium-gas flow cooling. The temperature was automatically controlled with a thermocouple sensor positioned close to the crystal, but out of the laser beam. A coherent single-mode argon-ion laser provided 200 mW (at the sample) at 514.5 nm. Scattered light was analyzed with a six-pass (4+2) homemade Sandercock-type tandem Fabry-Perot interferometer constructed in the D.R.P. shop. The piezoelectric-transducer scanning elements were controlled by a Commodore 64 microcomputer that was also used for storage of the data. The aperture used for collecting the scattered light was 2°. The plate separations (10, 11, 12, and 13 mm) were chosen so that the Brillouin lines were clearly visible in backscattering geometry even with intense scattered elastic light. The experimental setup is shown in Fig. 3.

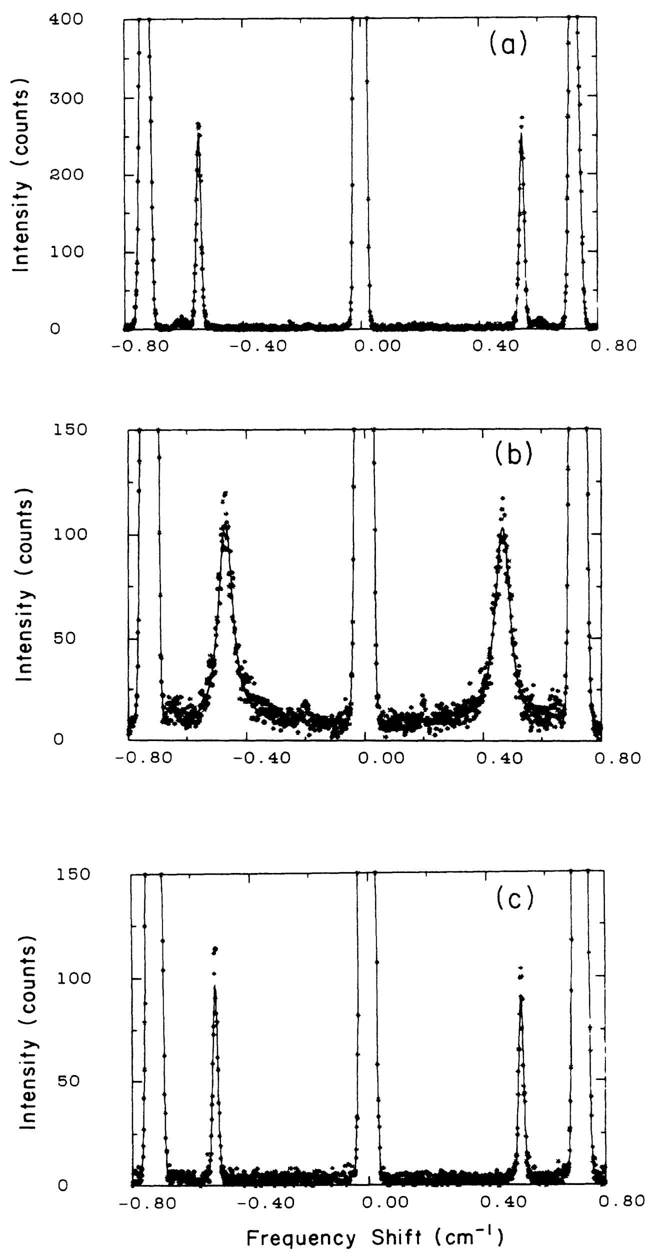

FIG. 2. Brillouin spectra of K_2SeO_4 in the $(a+c)[b,T](a-c)$ scattering geometry with $\theta = 90°$ at (top to bottom) (a) $T = 300$ K, (b) 127.5 K, and (c) 81 K showing the C_{33} longitudinal-acoustic mode.

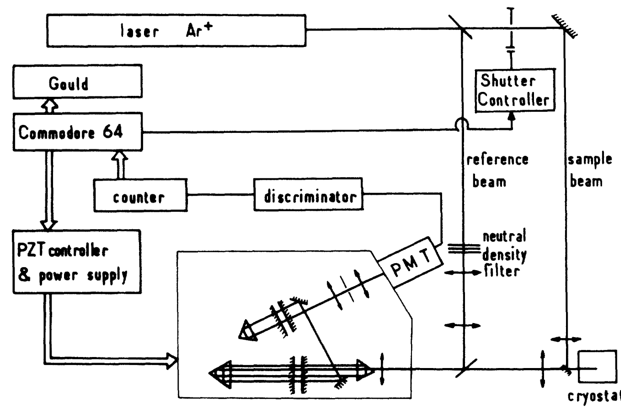

FIG. 3. Schematic illustration of the DRP six-pass tandem interferometer.

2 500 data channels were stored for 200 scans far from T_I and 400 scans near T_I. Data were transferred to a Gould minicomputer for subsequent analysis.

Figure 4 shows Brillouin spectra for three different temperatures: above, around, and below T_I. The broadening of the Brillouin lines near T_I is clearly visible.

The crystals used in the experiments in Paris and New York were subsequently exchanged and the experiments were repeated to insure the consistency of the results. In both experiments, the elastic constant $C'_{33}(\omega)$ and linewidth $\gamma_{33}(\omega)$ were obtained from damped harmonic-oscillator fits after deconvolution of the instrument function. In the analysis, we used $n_b = 2.539$ and $\rho_m = 3.05$ g cm^{-3}. The results for the 90° experiment are shown in Fig. 5.

VI. COMPARISON OF THEORY WITH EXPERIMENT

The data obtained in our Brillouin-scattering experiments described in Sec. V can now be compared with the mean-field theory predictions for $C'_{33}(\omega)$ and $\gamma_{33}(\omega)$ given in Eqs. (3.8)–(3.11). We begin by evaluating these equations using the free-energy coefficients derived in

Sec. IV. For the acoustic frequency ω in these equations we used the approximate value

$$\omega = \left[\frac{C_{33}^0}{\rho_m} \right]^{1/2} n_b \frac{\omega_L}{c} \sin(\theta/2) , \tag{6.1}$$

where ω_L is the laser frequency, c/n_b is the speed of light in the crystal, and θ is the scattering angle. This value of ω corresponds to the "bare" frequency of the acoustic phonon without including coupling.

We evaluated the equations both with $g_{33}=0$, $D\neq 0$, and vice versa. The results for the two cases were somewhat different for $C'_{33}(\omega)$ but were essentially identical for $\gamma_{33}(\omega)$.

Evaluation of the integrals appearing in the equations was carried out in several different approximations. For $T > T_I$, we first used the dispersion curve of $\Omega_2(\mathbf{q})$ determined by Iizumi *et al.*[3] and integrated over the full Bril-

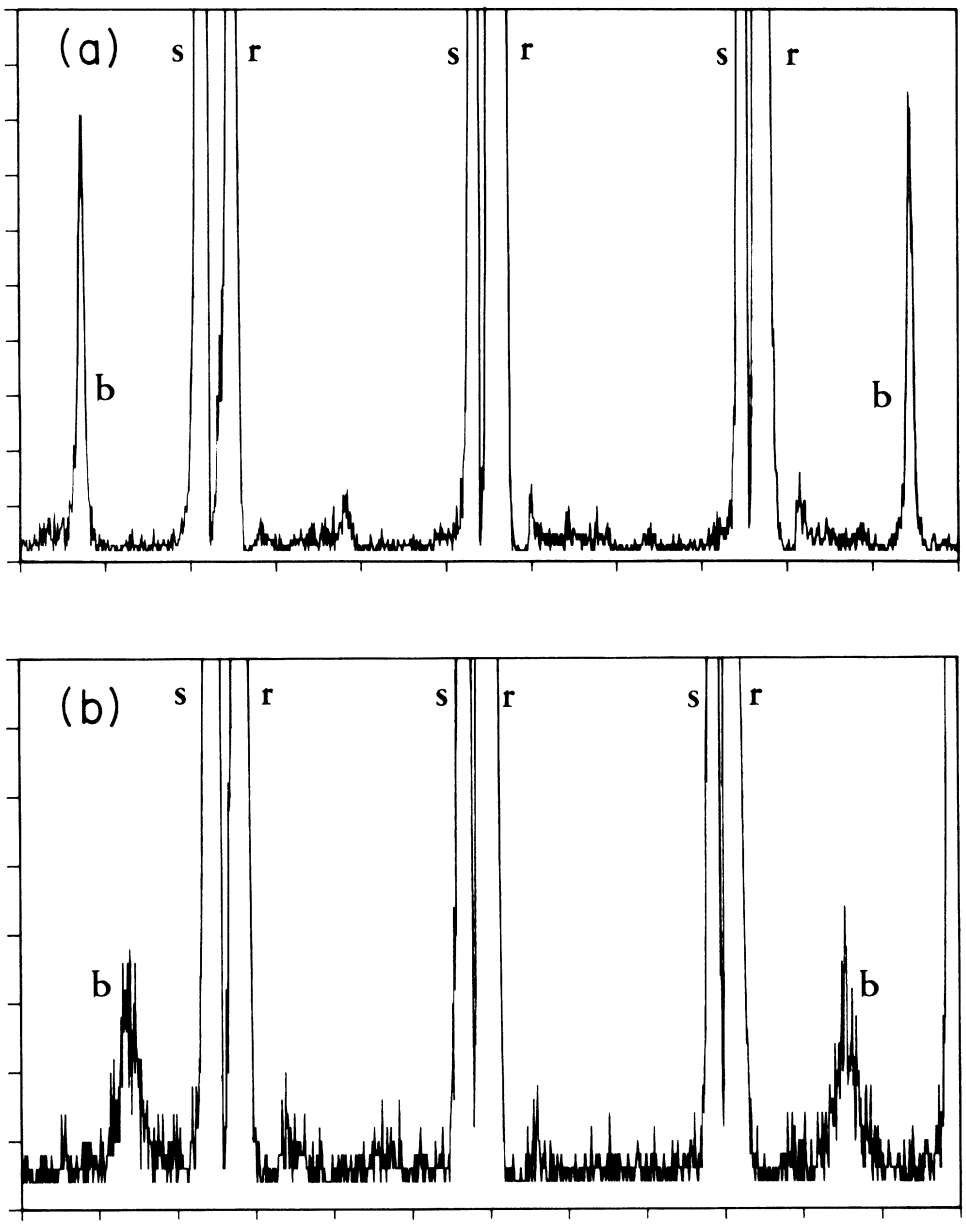

FIG. 4. Brillouin spectra of K_2SeO_4 in the $(\mathbf{c})[\mathbf{b},T](-\mathbf{c})$ scattering geometry with $\theta=180°$, at (top to bottom) (a) $T=134$ K, (b) 124.5 K, and (c) 117.5 K. (a): 100 channels=0.1566 cm^{-1} (FSR=0.4545 cm^{-1}), (b) and (c): 100 channels=0.1373 cm^{-1} (FSR=0.4255 cm^{-1}). *b* indicates the Brillouin components, *s* the elastic scattering from the sample. For a count rate exceeding a computer-defined value, the shutter is closed; a reference beam is still present producing the features labeled *R*.

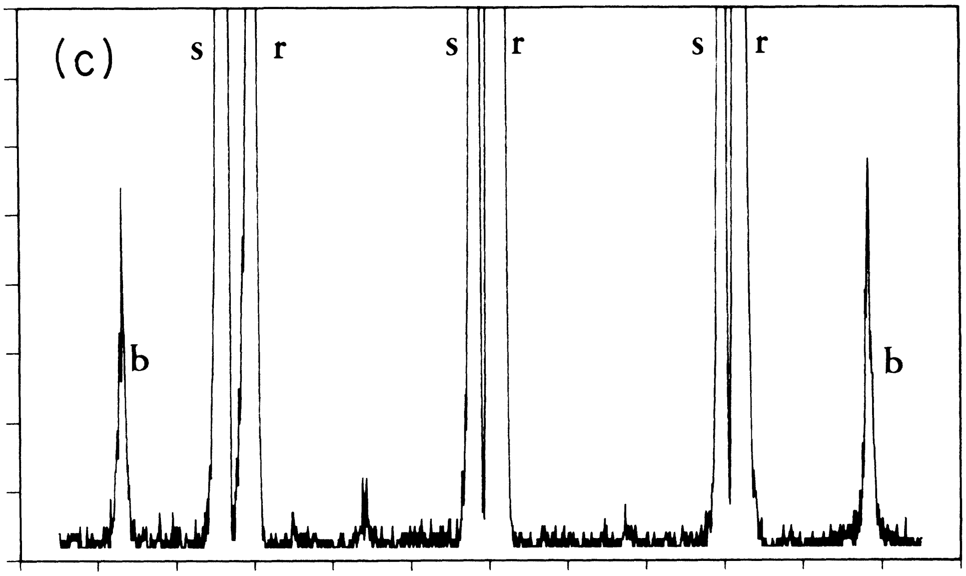

FIG. 4. (*Continued*).

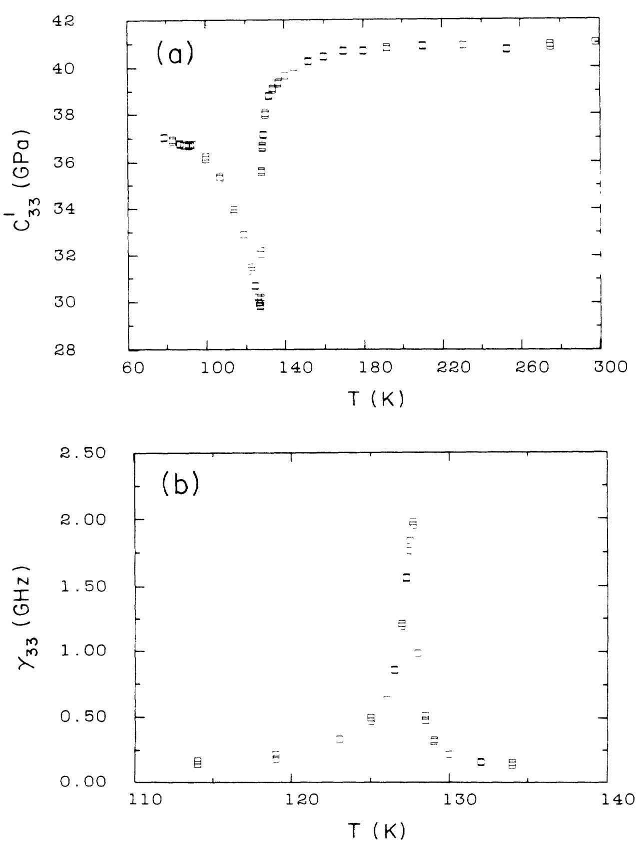

FIG. 5. Temperature dependences of (a) $C'_{33}(\omega)$ and (b) $\gamma_{33}(\omega)$ deduced from the 90° Brillouin-scattering data with damped harmonic-oscillator fits.

louin zone. We then used the parabolic approximation [Eq. (4.12)], integrated over a cylindrical volume with its axis along **a**, equal to one-half the volume of the Brillouin zone, and multiplied the result by 2. These two procedures gave results that were indistinguishable, and were insensitive to changes in the integration volume demonstrating that the integral is dominated by a small volume element centered at the minimum. Consequently, we used the second procedure for $T > T_I$, and also for $T < T_I$, without multiplication by 2.

The results of the evaluation are shown in Fig. 6 with $C'_{33}(\omega)$ on the left and $\gamma_{33}(\omega)$ on the right. The top pair of figures [Fig. 6(a)] are the first terms of Eqs. (3.8)–(3.11) ($C^0_{33}+2g\rho_0^2$ and γ^0_{33}), the second pair [Fig. 6(b)] are the Landau-Khalatnikov terms, and the third pair [Fig. 6(c)] are the anharmonic contributions found from the integrals. For reasons to be discussed below, we performed this calculation with three different values of the phason gap $\Omega_\phi(0)=0$, 60 GHz, and 160 GHz. The bottom pair [Fig. 6(d)] are the total $C'_{33}(\omega)$ and $\gamma_{33}(\omega)$ found by adding these three contributions. Clearly the size of the phason gap has only a minor effect on $C'_{33}(\omega)$, but causes major changes in the value of $\gamma_{33}(\omega)$ with a saturation effect for large values of $\Omega_\phi(0)$ that totally suppresses the phason contribution.

A comparison of Figs. 5 and 6 makes clear the importance of using a consistent theory. The rounding of $C'_{33}(\omega)$ and $\gamma_{33}(\omega)$ above T_I, which is very distinct in the experimental data (Fig. 5), cannot be obtained without including the fluctuation terms [Fig. 6(c)]. Conversely, once the contribution of both the phason and the amplitudon are taken into account, $\gamma_{33}(\omega)$ is too large below T_I in Fig. 6(c) if a phason gap is not introduced in the phason dispersion curve.

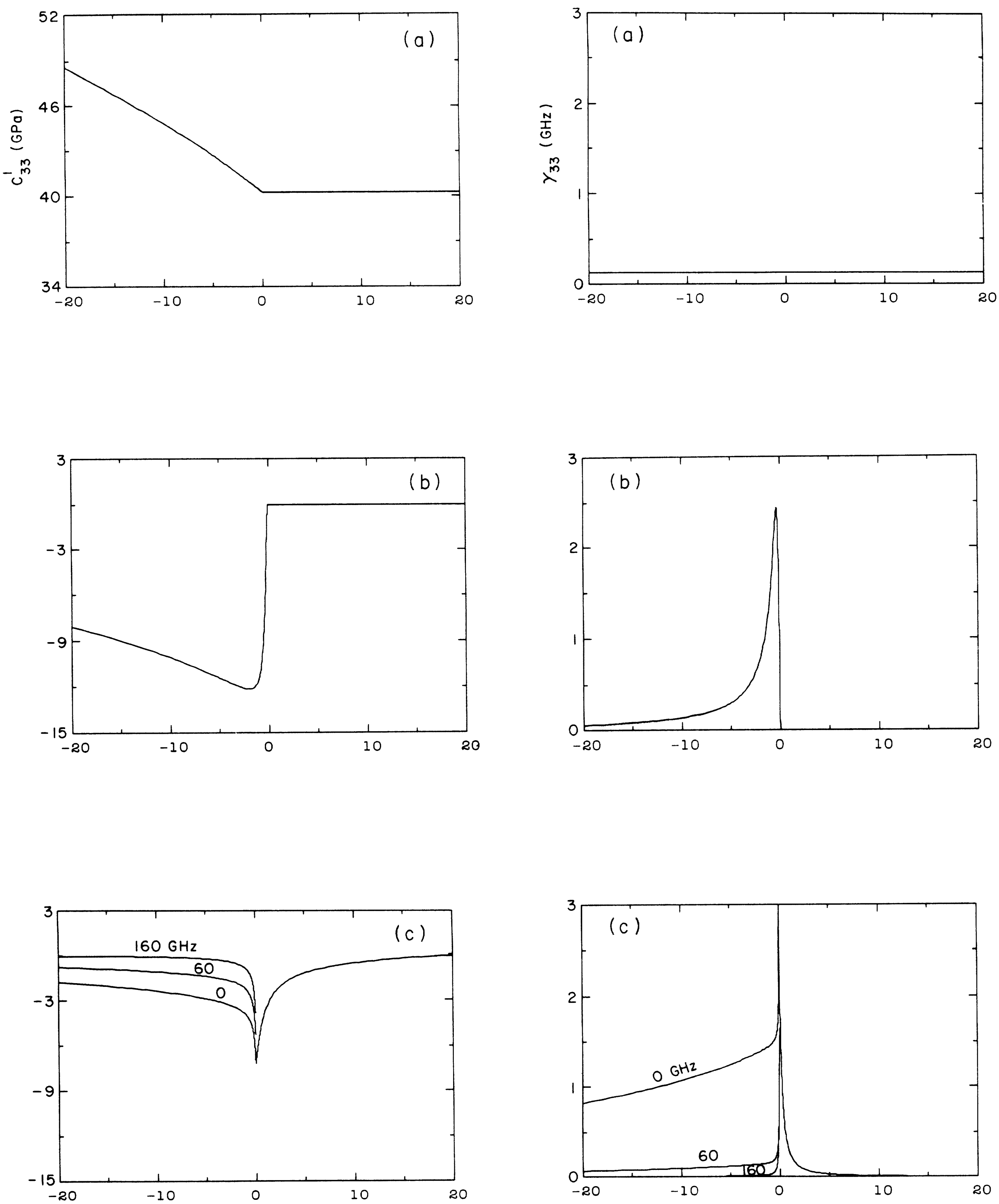

FIG. 6. Theoretical predictions for the anomaly in $C'_{33}(\omega)$ (left) and $\gamma_{33}(\omega)$ (right) predicted by Eqs. (3.8)–(3.11). The free-energy coefficients were determined from other experiments and are listed in the second column of Table I. The equations were evaluated with three values for the phason gap: $\Omega_\phi(0)=0$, 100, and 160 GHz. Top pair (a): the first terms of Eqs. (3.8)–(3.11). Second pair (b): the Landau-Khalatnikov contribution. Third pair (c): anharmonic contributions from third-order coupling to pairs of soft modes ($T > T_I$) or pairs of amplitudons or phasons ($T < T_I$). Bottom pair (d): total values.

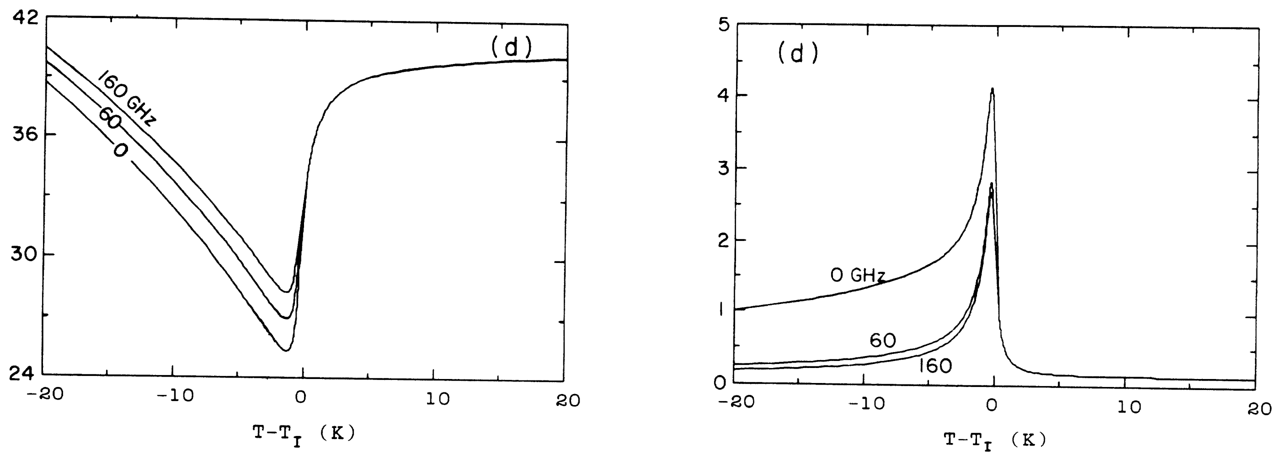

FIG. 6. (*Continued*).

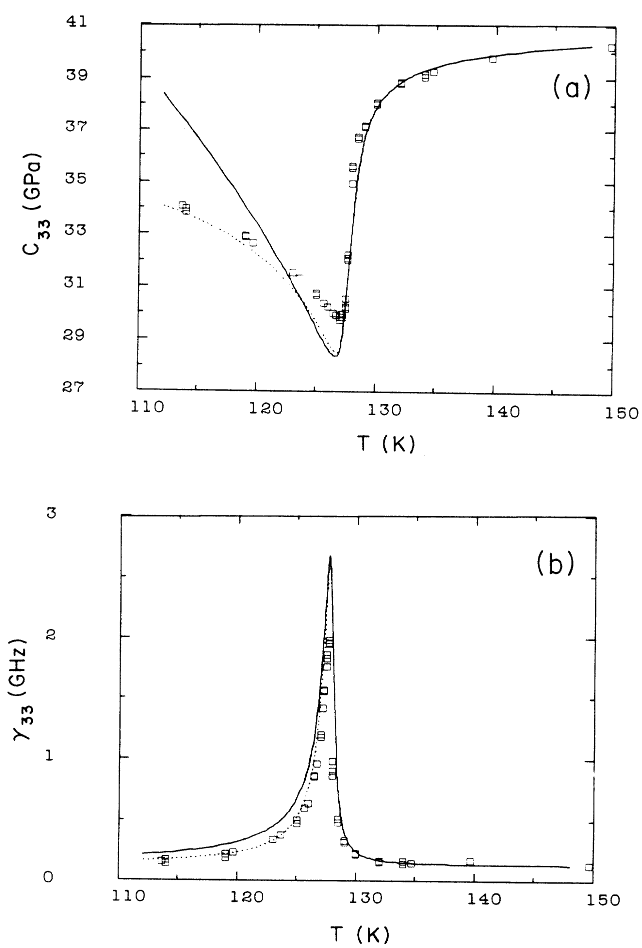

FIG. 7. Comparison of the 90° Billouin data of Fig. 5 with the theoretical predictions of Fig. 6 for (a) $C_{33}'(\omega)$ and (b) $\gamma_{33}(\omega)$. Solid lines, $D=0$. Dotted lines, $g_3=0$. The theoretical fits include a phason gap $\Omega_\phi(0)=160$ GHz. The free-energy coefficients used were those computed from the results of other experiments, listed in the second column of Table I.

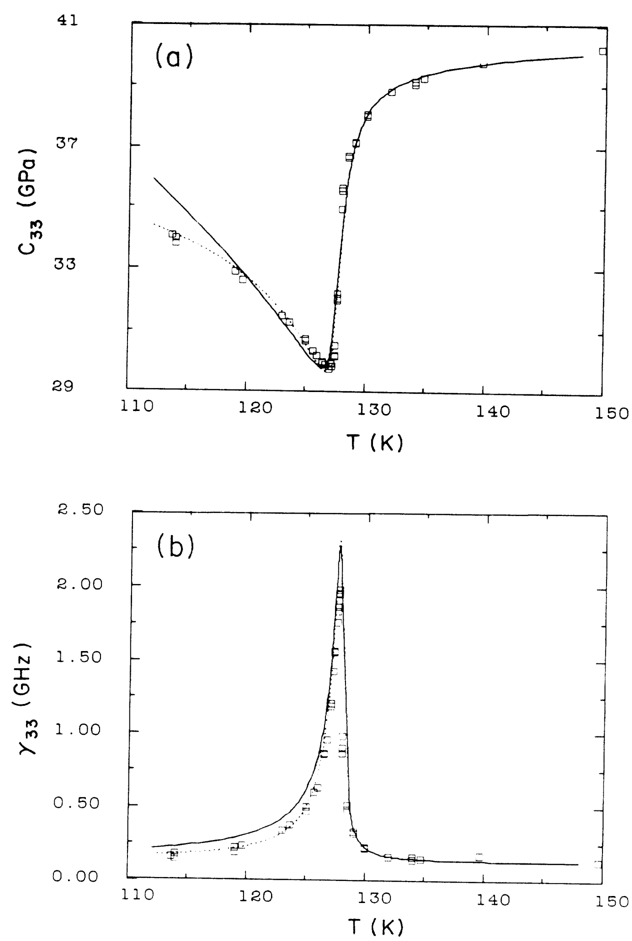

FIG. 8. Same as Fig. 7, but with the coefficients adjusted to simultaneously produce a best fit to both (a) $C_{33}'(\omega)$ and (b) $\gamma_{33}(\omega)$. The resulting adjusted values of the free-energy coefficients are listed in the third column of Table I. Note that fits are shown using either $D=0$ (solid lines) or $g_3=0$ (dashed lines) withe the $g_3=0$ fits giving better agreement.

In Fig. 7, our 90° results are compared with these theoretical predictions using 160 GHz for the phason gap. This value has been obtained indirectly by Topic in a recent NMR study of K_2SeO_4.[36] The agreement is fair, which is already important in view of the uncertainties in some of the numerical values we have used, but certainly not totally convincing.

Subsequently, we carried out a nonlinear least-squares fit in which B and h_3 as well as D (with $g_3=0$) or g_3 (with $D=0$) were varied in order to optimize the fit to the 90° data. In Fig. 8, we show the optimized fits obtained either with $g_3=0$ ($D\neq0$) or with $D=0$ ($g_3\neq0$). As can be seen, a better fit is obtained for the $g_3=0$ ($D\neq0$) case. The resulting values of the parameters are given in the third column of Table I. The small resulting changes in B, h_3 and D or g_3 are within the experimental accuracy.

The fits presented here have been obtained with $\Omega_\phi(0)=160$ GHz; other values larger than approximately 100 GHz would also be acceptable, producing only minor changes in the three adjusted parameters. Lower values would lead to too large values of $\gamma_{33}(\omega)$ at low temperature, in disagreement with our experimental data. Note that this lower limit on $\Omega_\phi(0)$ deduced from our experiments is slightly above the upper limit of 85 GHz deduced from Fig. 5 of Quilichini and Currat.[34]

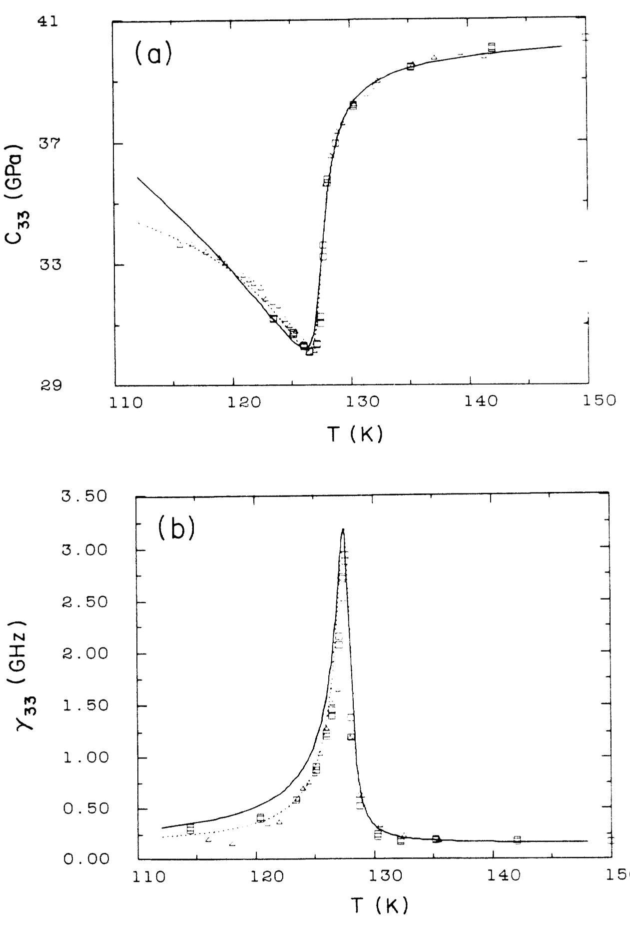

FIG. 9. Experimental (a) $C'_{33}(\omega)$ and (b) $\gamma_{33}(\omega)$ values from $\theta=180°$ backscattering experiments, together with theoretical curves computed with the same parameters used in Fig. 8. Data points are (△) Paris, (□) New York.

We have further checked our theoretical results against the 180° $C'_{33}(\omega)$ and $\gamma_{33}(\omega)$ data that has been measured by both groups. The comparison, shown in Fig. 9, is again quite convincing in the $g_3=0$ ($D\neq0$) case, showing that a consistent mean-field theory can explain all our experimental results, a nontrivial conclusion in view of the previous studies of this acoustic anomaly, as we shall see in Sec. VII.

VII. COMPARISON WITH PREVIOUS STUDIES

As mentioned in the Introduction, the $C_{33}(\omega)$ anomaly in K_2SeO_4 has been the subject of several previous experimental investigations. However, the analysis of the effect in all of these investigations was incomplete.

Yagi *et al.*[11] were the first group to study the C_{33} anomaly near T_I in their Brillouin-scattering determination of $C'_{33}(\omega)$. In their theoretical analysis they used the same free-energy expansion given in Eq. (2.1), adding a term $\delta_3\epsilon_3\rho^4$ for completeness.

Their analysis included both the bilinear-coupling contribution [Eq. (3.2) in the static limit] and the anharmonic contribution, but with all coefficients treated as adjustable parameters. In their evaluation of the second contribution, they did not consider either the $\mathbf{q}_0, -\mathbf{q}_0$ degeneracy of the soft mode above T_I, or the role of phasons below T_I. In their analysis they assumed that the soft-mode dispersion curve is isotropic, and that $\rho_0(T)$ is always small enough so that all equations can be linearized in $(T-T_I)$.

They found reasonable agreement between their theoretical expressions and their experimental results. However, in view of the assumptions made in deriving their equation for $C'_{33}(\omega)$ [Eq. (11) in their paper] and the fact that the linewidth was not analyzed, the values they found for the coefficients cannot be expected to be physically significant.

Rehwald *et al.*[5] compared ultrasonic and Brillouin data for $C'_{33}(\omega)$ and were the first to measure $\gamma_{33}(\omega)$. They also presented a careful theoretical analysis of the harmonic contributions to $C'_{33}(\omega)$. They pointed out a further coupling of C_{33} to the phason and to the amplitudon at $\mathbf{K}=\delta\mathbf{a}^*$ arising from a $p_3\epsilon_3\rho^3$ term, linearized to $p_3\epsilon_3\rho_0^2\rho$ below T_I. They concluded that this effect was presumably too small to be measured and did not attempt any fit.

Hauret and Benoit[12] determined both $C'_{33}(\omega)$ and $\gamma_{33}(\omega)$ in a 90° Brillouin-scattering experiment. They analyzed their data in the framework of Eq. (2.1) setting $D=0$, but considered only the Landau-Khalatnikov term, ignoring anharmonic effects. Since this procedure did not enable them to take into account the rounding off of $C'_{33}(\omega)$ above T_I, they deduced a value for T_I from their data and assumed that the analysis is valid below that temperature. Fitting their results to Eq. (3.3), they deduced a relaxation time $\tau=\tau_0(T_I-T)^{-1}$ with

$\tau_0=2.6\times10^{-12}$ s, in fair agreement with our value $\tau_0=2.1\times10^{-12}$ s obtained from Table I. Having set $D=0$, they could not explain the downward curvature of $C'_{33}(\omega)$ below T_I in the $\omega\tau\ll1$ regime, and had to use a non-mean-field critical exponent for $\rho_0(T)$ ($2\beta\sim0.75$) in order to achieve a reasonable fit through the $g_3\rho_0^2(T)$ term of Eq. (3.10). This group[13] subsequently performed additional Brillouin-scattering experiments at 45°, 90°, and 135°, which illustrated the ω dependence of $\tilde{C}_{33}(\omega)$. They confirmed their previous value of $\tau_0=(2.85\pm0.20)10^{-12}$ s.

Esayan and Lemanov[23] performed ultrasonic measurements, and were the first to take into account the role of the $\mathbf{K}\approx\mathbf{0}$ phason. Remaining again within the Landau-Khalatnikov approximation, they simply mentioned the absence of coupling of the strain ϵ_3 to this excitation.

Finally, we note that a recent Brillouin-scattering study of Rb_2ZnBr_4 and Rb_2ZnCl_4 by Horikx *et al.*[37] employed an analysis very similar to that presented here. They included both the Landau-Khalatnikov and anharmonic fluctuation terms, but did not include phason contributions. Since inelastic-neutron-scattering studies of these materials have not shown any propagating soft modes,[38–40] their fits could not be carried out using independent dynamical data as inputs. Furthermore, the elastic anomalies in these materials are very weak compared to the strong C_{33} anomaly in K_2SeO_4 making the analysis much less significant.

VIII. SUMMARY AND DISCUSSION

In this paper, we have presented a reanalysis of the anomaly of the elastic constant $\tilde{C}_{33}(\omega)$ of K_2SeO_4 in the vicinity of the normal-incommensurate second-order phase transition at $T_I=127.5$ K. This analysis has been performed in the framework of a consistent mean-field theory. Having developed the relevant dynamical free energy, we have systematically treated the most significant coupling terms between the elastic strain ϵ_3 and the dynamical variables belonging to the Σ_2 phonon branch that becomes soft at T_I at the incommensurate wave vectors $\pm\mathbf{q}_0$. We have found that the anharmonic coupling of ϵ_3 with two excitations in the vicinity of $\mathbf{q}=\mathbf{q}_0$ in the incommensurate phase had not been properly considered previously: coupling to two phase modes has to be taken into account on the same basis as coupling to two amplitude modes. Both effects give rise to a decrease of $C'_{33}(\omega)$ and contribute to $\gamma_{33}(\omega)$; the phason coupling is particularly important for $\gamma_{33}(\omega)$.

We evaluated the various coefficients appearing in the free-energy expansion using available static and dynamical data, and analyzed all of them in the same mean-field spirit.

A detailed analysis of the values of $C'_{33}(\omega)$ and $\gamma_{33}(\omega)$ determined from our 90° and 180° Brillouin-scattering experiments has shown an excellent agreement with the theoretical predictions. This agreement was achieved with only minor adjustments of some of the free-energy coefficients. It was nevertheless necessary to include a phason gap that we took as temperature independent. We found a lower limit for this gap of ~100 GHz that is slightly above the value found from neutron-scattering experiments. We stress that a $\mathbf{K}=0$ gap in the excitation spectrum of the phason is not predicted by the mean-field theory; it had to be inserted as an additional assumption.

Furthermore, there is extensive evidence of other deviations from the mean-field approximation. For instance, Majkrzak *et al.*[41] analyzed the temperature dependence of the primary neutron-diffraction modulation satellites of K_2SeO_4, which they fit to $I(T)\propto(T_I-T)^{2\beta}$ and found $2\beta\cong0.75$. The temperature dependence of the soft-mode frequency in K_2SeO_4 (Fig. 7 of Ref. 3), which should behave as $\Omega_2^2(\mathbf{q}_0)\propto(T-T_I)^\gamma$, clearly shows upward curvature indicative of $\gamma>1$ rather than the $\gamma=1$ behavior used in our mean-field analysis $[\Omega_2^2(\mathbf{q}_0)=\frac{1}{2}A_0(T-T_I)]$. Andrews and Mashiyama[42] studied diffuse x-ray scattering in the K_2SeO_4 isomorph Rb_2ZnCl_4 and found critical exponents $\beta=0.345$, $\gamma=1.26$, and $\nu=0.693$. These results are in clear disagreement with the mean-field prediction $\beta=\frac{1}{2}$, $\gamma=1$, and $\nu=\frac{1}{2}$. In the incommensurate phase of K_2SeO_4, Unruh *et al.*[43] have found that the dielectric anomaly behaves as $\Delta\chi\sim(T_I-T)^{0.76}$, while the amplitude-mode frequency $\Omega_A^2(0)\sim(T_I-T)^{0.52}$. They also found that Γ_A, the damping constant for the amplitude mode deduced from Raman data, increases strongly near T_I.[44] We found their results to be well described by

$$\Gamma_A=\left[-0.089(T_I-T)+9.6+\frac{300}{(T_I-T)^2+21}\right]\text{cm}^{-1}\,. \tag{8.1}$$

To proceed with our analysis beyond the mean-field approximation would require a complete theory that does not yet exist, although some ingredients are already available. Because K_2SeO_4 is a 3D system with a doubly degenerate soft mode, its critical properties should be those of the 3D *XY* ferromagnet for which theoretical estimates are available. Le Guillou and Zinn-Justin,[45] for example, have found for this ($d=3$, $n=2$) universality class, $\gamma=1.316$, $\beta=0.3455$, and $\nu=0.669$, in good agreement with the results of Andrews and Mashiyama.[42] The extent of the critical region and the importance of corrections to scaling in this class of materials has not yet been investigated, nor have the consequences of non-mean-field behavior for the lattice dynamics been explored.

Some of the groundwork for a scaling analysis of the acoustic anomalies in incommensurate crystals has been developed by Schwabl and his co-workers[46,47] (also see Luthi and Rehwald[48]), and some ultrasonic studies of phase transitions have already been analyzed with scaling arguments, such as the $NaNO_2$ experiments reported by Hu *et al.*[49] Schwabl has also noted that the separation of the acoustic anomaly into Landau-Khalatnikov and anharmonic contributions may not be correct in the context of a scaling theory.[47,50]

In the absence of a complete theory, there is no straightforward way to carry out an analysis of the acoustic anomaly beyond the mean-field approximation. In general, one cannot modify the temperature dependence of any property without simultaneously changing others.

As an example, we repeated the analysis shown in Fig. 8 with the amplitude-mode damping constant Γ_A found by Unruh *et al.* [Eq. (8.1)] rather than the T-linear form [Eq. (4.13)] used previously, with $\Omega_A^2(0)$ given by Eq. (4.14), and with the free-energy coefficients adjusted to optimize the fit. The resulting fit showed very poor agreement with the data as shown by the solid curves in Fig. 10. We therefore also included a nonclassical amplitudon frequency $\Omega_A^2(0) \propto (T_I - T)^\gamma$ in the Landau-Khalatnikov term [the second term in Eq. (3.10)] with γ as a free parameter. The result, also shown in Fig. 10 by the dotted lines, is in much closer agreement with experiment, but the fit gave $\gamma = 0.66$ rather than $\gamma = 0.52$ found by Unruh *et al.*[43]

Finally, we note that in our formulation of the theory, the anharmonic terms are treated in lowest order through cubic coupling of acoustic phonons to pairs of soft modes above T_I or to pairs of amplitudons or phasons below T_I [first term in Eq. (2.5)]. Recently, however, Levanyuk[51] has found that the higher-order anharmonic terms in Eq. (2.3) also contribute significantly in the incommensurate phase, leading to renormalization of the temperature-dependent coupling coefficients that multiply the fluctuation integrals in Eqs. (3.10) and (3.11). Although such effects may well modify some of the conclusions of our analysis, their formulation is not yet sufficiently complete for carrying out a quantitative analysis of the experimental data.

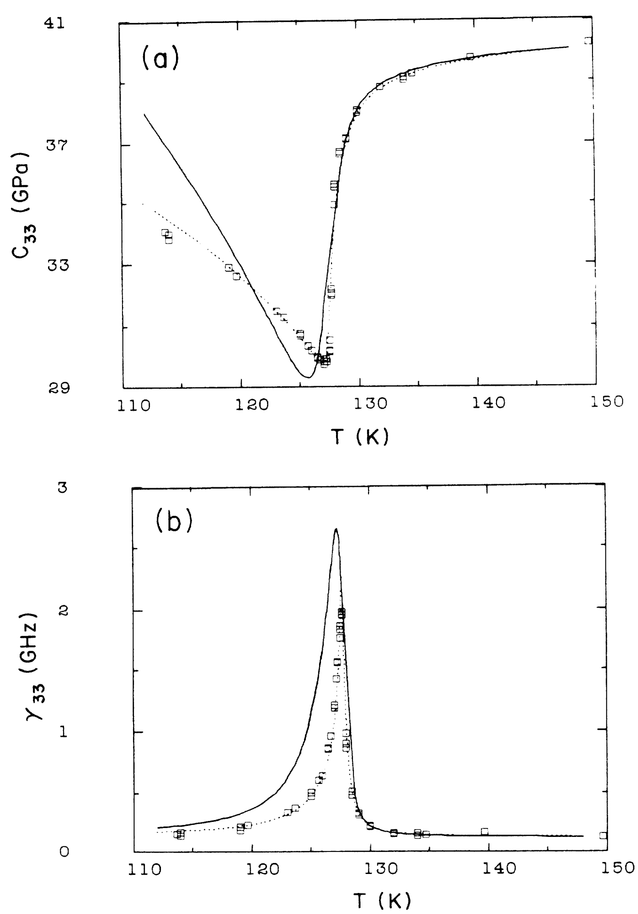

FIG. 10. Fits to (a) $C'_{33}(\omega)$ and (b) $\gamma_{33}(\omega)$ using Unruh's amplitudon damping constant from Eq. (8.1). Solid lines: best fit with mean-field amplitudon frequency. Dotted lines denote best fit obtained with $\Omega_A^2(0) \propto (T_I - T)^\gamma$. The fitting results were $\gamma = 0.66$, $B = 2.5 \times 10^{42}$ g^{-1}cm s^{-2}, $h_3 = 3.8 \times 10^{26}$ s^{-2} and $g_3 = 0.72 \times 10^{-28}$ s^{-2} (with $D = 0$).

Note: Recently, a paper by Chen appeared [Phys. Rev. B **41**, 9516 (1990)] in which the K_2SeO_4 specific-heat data was reanalyzed and shown to agree very closely with the predictions of the 3D *XY* model.

ACKNOWLEDGMENTS

We wish to thank C. Garland, R. Griffiths, A. P. Levanyuk, H. Poulet, and F. Schwabl for helpful discussions; A. Marillier for assistance with the electronics of the Paris interferometer, G. Hauret for providing the crystals, and N. Lenain for sample preparation. Support for the work at City College of the City University of New York (CCNY) was provided by the U.S. National Science Foundation under Grant No. DMR-8614168. Support for this program at the University P. and M. Curie was provided in part by The Direction Des Recherches Etudes et Techniques–Ministere De La Defense (DRET) Contract No. 85.1333. Travel funds for this collaboration were supplied by The Scientific Affairs Division of The North Atlantic Treaty Organization (NATO) through Research Grant No. 86-0283.

APPENDIX A: THE LANDAU FREE-ENERGY FUNCTIONAL $f(x)$

The Landau free-energy functional $f(x)$ for K_2SeO_4 can be expressed as a sum of three parts:[52]

$$f(x) = f_Q(x) + f_\epsilon(x) + f_P(x) , \tag{A1}$$

where $f_Q(x)$ includes terms only in the order parameter Q, which is the complex position-dependent amplitude of the Σ_2 mode at the commensurate wave vector $\mathbf{q}_c = \mathbf{a}^*/3$, $f_\epsilon(x)$ includes terms in the strains ϵ_i ($i = 1-6$) both alone and in combination with Q, and $f_P(x)$ includes terms in the polarization P_3 both alone and in combination with Q:

$$f_Q(x) = \tfrac{1}{2}\alpha QQ^* + \tfrac{1}{4}\beta'(QQ^*)^2 + \tfrac{1}{6}\gamma_1'(QQ^*)^3 - i\frac{\sigma}{2}\left[Q\frac{dQ^*}{dx} - Q^*\frac{dQ}{dx}\right] + \frac{\kappa}{2}\frac{dQ^*}{dx}\frac{dQ}{dx} + \tfrac{1}{2}\gamma'(Q^6 + Q^{*6}) \tag{A2}$$

$$f_P(x) = \frac{1}{2\chi_0}P^2 + \frac{\eta}{2}P^2QQ^* + i\xi P(Q^3 - Q^{*3}) - PE , \tag{A3}$$

$$f_\epsilon(x) = \tfrac{1}{2}\sum_{i,j=1}^{6} C_{ij}\epsilon_i\epsilon_j - \sum_{j=1}^{3} h_j\epsilon_j QQ^* + \sum_{i,j=1}^{3} g_{ij}\epsilon_i\epsilon_j QQ^* + \sum_{i=4}^{6} g_i\epsilon_i^2 QQ^* + \tfrac{1}{2}a_5\epsilon_5(Q^3 + Q^{*3}) - \sum_{i-1}^{6}\epsilon_i\sigma_i \tag{A4}$$

where $\alpha=\alpha_0(T-T_0)$ and all other coefficients are assumed to be temperature independent. To simplify $f(x)$, we first make the usual transformation to polar coordinates $Q=\rho e^{i\phi(x)}$, and invoke the continuum constant-amplitude approximation $d\rho/dx=0$. Since we will not consider the polarization P we minimize the average free-energy density $F=(1/L)\int_0^L f(x)\,dx$ with respect to P to find its equilibrium value, and eliminate it from $F(x)$ assuming that the electric field E and the stresses σ_i are zero. This process modifies the coefficients γ', γ'_1, and β'.

Minimization of the resulting expression with respect to ϕ shows that near T_I, where ρ is small, $d\phi/dx$ is a constant independent of x, which we take as $q-q_c$. Ignoring all strains except ϵ_1, ϵ_2, ϵ_3, and the off-diagonal components of g_{ij} then gives an approximate form for $f(x)$:

$$f(x)\cong\tfrac{1}{2}[\alpha-2\sigma(q-q_c)+\kappa(q-q_c)^2]\rho^2+\tfrac{1}{4}\beta\rho^4+\tfrac{1}{6}\gamma_1\rho^6+\tfrac{1}{2}\sum_{i,j=1}^{3}C_{ij}\epsilon_i\epsilon_j-\sum_{i=1}^{3}h_i\epsilon_i\rho^2+\sum_{i=1}^{3}g_i\epsilon_i^2\rho^2\ . \tag{A5}$$

This is just the incommensurate-plane-wave limit; ρ is the amplitude of a Σ_2 mode at the (still unspecified) wave vector q, and $f(x)$ of Eq. (A5) is thus the free-energy density of a single mode. Minimization of $f(x)$ with respect to q gives

$$q=q_0=q_c+\frac{\sigma}{\kappa}$$

so that, with $q=q_0$,

$$f(x)\cong\frac{1}{2}\left[\alpha-\frac{\sigma^2}{\kappa}\right]\rho^2+\tfrac{1}{4}\beta\rho^4+\tfrac{1}{2}\sum_{i,j=1}^{6}C_{ij}\epsilon_i\epsilon_j-\sum_{i=1}^{3}h_i\epsilon_i\rho^2+\sum_{i=1}^{3}g_i\epsilon_i^2\rho^2\ . \tag{A6}$$

Note that the Lifshitz invariant term $-i(\sigma/2)[Q(dQ^*/dx)-Q^*(dQ/dx)]$ in Eq. (A2) shifts the minimum in the part of $f(x)$ quadratic in ρ from $\mathbf{q}_c=\mathbf{a}^*/3$ to $\mathbf{q}_0$, and also increases the transition temperature from T_0, where $\alpha=\alpha_0(T-T_0)\rightarrow 0$ (the virtual paracommensurate transition) to $T_I=T_0+(\sigma^2/\alpha_0\kappa)$, where $[\alpha-(\sigma^2/\kappa)]\rightarrow 0$.

Finally, replacing $[\alpha-(\sigma^2/\kappa)]$ by $A=A_0(T-T_I)$ and β by B and noting that $f(x)$ is no longer dependent on x and is therefore identical to the average free-energy density F, we have (approximately, neglecting shear strains)

$$F=\tfrac{1}{2}A_0(T-T_I)\rho^2+\tfrac{1}{4}B\rho^4+\tfrac{1}{6}D\rho^6+\tfrac{1}{2}\sum_{i,j}^{3}C_{ij}\epsilon_i\epsilon_j-\sum_{i=1}^{3}h_i\epsilon_i\rho^2+\sum_{i=1}^{3}g_i\epsilon_i^2\rho^2\ , \tag{A7}$$

which is the approximate form of the free energy given in Eq. (2.1) in the text.

APPENDIX B

The complex elastic constant $\tilde{C}_{33}(\omega)$ can be obtained from the free energy given in Eqs. (2.2)–(2.5) using standard techniques of anharmonic phonon theory. The 3×3 dynamical matrix for acoustic phonons may be written as

$$\|M_{\alpha\beta}\|=\left\|\frac{1}{\rho_m}\sum_{\gamma,\delta}\tilde{C}_{\alpha\gamma,\beta\delta}(\omega)q_\gamma q_\delta-\omega^2\delta_{\alpha\beta}\right\|=\left\|\frac{1}{\rho_m}\left[\sum_{\gamma,\delta}C^0_{\alpha\gamma,\beta\delta}q_\gamma q_\delta+\Sigma_{\alpha\beta}(\mathbf{q},\omega)\right]-\omega^2\delta_{\alpha\beta}\right\|\ , \tag{B1}$$

where ρ_m is the mass density and $\Sigma_{\alpha\beta}(\mathbf{q},\omega)$ the self-energy tensor whose origin is related to the coupling term [Eq. (2.5)]. This term, as stated in Sec. III, does not play the same role above and below T_I, and we need to discuss the two situations in turn.

1. The $T>T_I$ case

At the lowest order in perturbation and for harmonic $Q(\mathbf{q})$ phonons, since the frequency of an acoustic phonon is always much smaller than $\Omega(\mathbf{q})$, the only damping mechanism is related to the first term of Eq. (2.5):

$$F_c^1=\frac{i}{\sqrt{\rho_m}}\sum_{\alpha,\mathbf{q}_1,\mathbf{q}_2,\mathbf{q}}h_{\alpha\alpha}(-\mathbf{q},-\mathbf{q}_1,-\mathbf{q}_2)q_\alpha U_\alpha(-\mathbf{q})\times Q(-\mathbf{q}_1)Q(-\mathbf{q}_2)\delta(\mathbf{q}+\mathbf{q}_1+\mathbf{q}_2)\ , \tag{B2}$$

where we have made explicit the wave-vector dependence of the elastic strain and used the acoustic-phonon coordinates. This damping mechanism is one in which an acoustic phonon with wave vector $\mathbf{q}$ and a $\mathbf{q}_1$ (or $\mathbf{q}_2$) other phonon are simultaneously destroyed and a third phonon with wave vector $-\mathbf{q}_2$ (or $-\mathbf{q}_1$) is created, with wave-vector conservation, followed by the reverse process. Such a mechanism may be represented by the usual bubble diagram and leads to the well known result:

$$\Sigma_{\alpha\beta}(\mathbf{q},\omega)=-\frac{\hbar}{2}\sum_{\mathbf{q}_1,\mathbf{q}_2}\frac{h_{\alpha\alpha}(-\mathbf{q},-\mathbf{q}_1,-\mathbf{q}_2)q_\alpha h_{\beta\beta}(\mathbf{q},\mathbf{q}_1,\mathbf{q}_2)q_\beta}{\Omega_1\Omega_2}\times[n(\Omega_2)-n(\Omega_1)]\left[\frac{1}{\omega+\Omega_1-\Omega_2}-\frac{1}{\omega-\Omega_1+\Omega_2}\right]\delta(\mathbf{q}+\mathbf{q}_1+\mathbf{q}_2)\ , \tag{B3}$$

where Ω_1 (resp. Ω_2) is the phonon frequency associated with the wave vector $\mathbf{q}_1$ (resp. $\mathbf{q}_2$) and $n(\Omega)$ the corresponding Bose-Einstein factor.

The situation is more complex in the case where $Q(\mathbf{q})$ corresponds to soft phonons the frequencies of which go to zero at $T=T_I$, for $\mathbf{q}=\epsilon\mathbf{q}_0$, $\epsilon=\pm 1$.

First, in Eq. (B3), the main contribution comes from wave vectors $\mathbf{q}_1$, which are in the vicinity of a minimum of the soft phonon dispersion curve: $\mathbf{q}_1=\epsilon\mathbf{q}_0+\mathbf{K}$, ($|\mathbf{K}|<|\mathbf{q}_0|$); due to the $\delta(\mathbf{q}+\mathbf{q}_1+\mathbf{q}_2)$ term, $-\mathbf{q}_2$ is also in the vicinity of $\epsilon\mathbf{q}_0$, while, if one neglects the wave-vector dependence of $h_{\alpha\alpha}$ in the vicinity of such a minimum,

$$h_{\alpha\alpha}(\mathbf{q},\epsilon\mathbf{q}_0+\mathbf{K},-\epsilon\mathbf{q}_0-\mathbf{K}-\mathbf{q}) \simeq h_{\alpha\alpha}(\mathbf{q},-\epsilon\mathbf{q}_0+\mathbf{K},\epsilon\mathbf{q}_0-\mathbf{K}-\mathbf{q})\equiv h^0_{\alpha\alpha}\equiv h_\iota \ . \tag{B4}$$

Consequently, the summation over $\mathbf{q}_1$ in Eq. (B3) is equivalent to twice a summation over $\mathbf{K}$ in the vicinity of one of the two minima only.

Second, as explained in Sec. III, the phonons on the Σ_2 branch are always damped, with a damping constant Γ much larger than the acoustic-phonon frequency, and also larger than the soft-mode frequencies in the vicinity of T_I, close to $\epsilon\mathbf{q}_0$. The bare phonon propagators,

$$P^0(\mathbf{q},\omega)=\frac{1}{\Omega^2(\mathbf{q})-\omega^2} \ , \tag{B5a}$$

which entered in the bubble diagram and led to Eq. (B3), have to be replaced by propagators related to (over)damped phonons:

$$P(\mathbf{q},\omega)=\frac{1}{\Omega^2(\mathbf{q})-i\omega\Gamma(\mathbf{q})-\omega^2} \ . \tag{B5b}$$

If one neglects, in the equations leading to Eq. (B3), the difference between $\Omega(\mathbf{q}_1)$ and $\Omega(\mathbf{q}_2)$ (because of the small value of $|\mathbf{q}|$), replaces the Bose Einstein factor $n(\Omega)$ by its classical limit, $(k_BT/\hbar\Omega)$, and integrates over the whole frequency spectrum implied by $P(\mathbf{q},\omega)$, one obtains the simplified result given by Levanyuk,[18] and Ginsburg et al.[53] which in the present case reads:

$$\Sigma_{\alpha\beta}(\mathbf{q},\omega)=-2k_BT(h^0_{\alpha\alpha}q_\alpha)(h^0_{\beta\beta}q_\beta) \times\sum_{\mathbf{K}}\frac{1}{\Omega^2(\mathbf{K})\left[\Omega^2(\mathbf{K})-\frac{i\omega}{2}\Gamma(\mathbf{K})\right]} \ . \tag{B6}$$

In obtaining this expression, we have supposed that the acoustic phonon frequency ω is much smaller than the soft-mode frequency and damping constant [$\omega\ll\Omega(\mathbf{K})$, $\Gamma(\mathbf{K})$]; also, $\mathbf{K}$ stands for $\mathbf{q}_1-\epsilon\mathbf{q}_0$ and the result has to be multiplied by 2 to take into account the existence of the two minima.

2. The $T<T_1$ case

Below the phase transition, the situation becomes more complex for two different reasons. Both $\langle Q(\mathbf{q}_0)\rangle$ and $\langle e_i\rangle$ $(i=1,2,3)$ have nonzero values, which can be, at each temperature, obtained from the minimization of Eq. (2.1). Furthermore, the dynamics of the soft mode is more complex, since it involves the amplitudon and the phason, and the different role of these two variables has to be taken into account.

a. Harmonic part of the free energy

Once the equilibrium values ρ_0 and ϵ^0_i are obtained, the harmonic part of the free energy may be easily computed by first taking the second derivatives of the free energy with respect to the dynamical variables that appear in Eqs. (2.2)–(2.5) and, second, replacing in these second derivatives all the remaining variables by their equilibrium values. Taking into account the equilibrium condition $(\partial F_{\rm eq}/\partial\rho_0)=(\partial F_{\rm eq}/\partial\epsilon^0_i)=0$, after some tedious but straightforward manipulations, one obtains:

$$\begin{aligned}F_{\rm harm}=\tfrac{1}{2}\sum_{\epsilon,\mathbf{K}}[&N(-\epsilon\mathbf{q}_0-\mathbf{K},\epsilon\mathbf{q}_0+\mathbf{K})Q(-\epsilon\mathbf{q}_0-\mathbf{K})Q(\epsilon\mathbf{q}_0+\mathbf{K})+R(\epsilon\mathbf{q}_0-\mathbf{K},\epsilon\mathbf{q}_0+\mathbf{K})Q(\epsilon\mathbf{q}_0-\mathbf{K})Q(\epsilon\mathbf{q}_0+\mathbf{K})\\&+\sum_{\mathbf{q},\alpha}H_\alpha(-\mathbf{q},\epsilon\mathbf{q}_0+\mathbf{K})U_\alpha(-\mathbf{q})Q(\epsilon\mathbf{q}_0+\mathbf{K})\delta(\mathbf{q}-\mathbf{K})]\\&+\frac{1}{2\rho_m}\sum_{\mathbf{q},\alpha,\ldots,\delta}(C^0_{\alpha\gamma,\beta\delta}+2g_{\alpha\beta}\delta_{\alpha\beta}\delta_{\gamma\delta}\rho_0^2)q_\gamma q_\delta U_\alpha(-\mathbf{q})U_\beta(\mathbf{q})\end{aligned} \tag{B7}$$

with

$$N(-\epsilon\mathbf{q}_0-\mathbf{K},\epsilon\mathbf{q}_0+\mathbf{K})=\omega^2(\rho)+\tfrac{1}{2}\sum_{\alpha,\beta}\Lambda_{\alpha\beta}K_\alpha K_\beta \ , \tag{B8a}$$

$$R(\epsilon\mathbf{q}_0-\mathbf{K},\epsilon\mathbf{q}_0+\mathbf{K})=\omega^2(\rho^2)e^{-2i\epsilon\varphi} \ , \tag{B8b}$$

$$\omega^2(\rho)=B\rho_0^2+2D\rho_0^4 \ , \tag{B8c}$$

$$H_\alpha(-\mathbf{q},\epsilon\mathbf{q}_0+\mathbf{K}) =i\sqrt{2/\rho_m}(h^0_{\alpha\alpha}-2\epsilon^0_i\delta_{i\alpha}g_{\alpha\alpha})q_\alpha\rho_0e^{-i\epsilon\varphi} \ , \tag{B9}$$

with $\epsilon=\pm1$,

$$\Lambda_{\alpha\beta}\equiv\begin{bmatrix}\Lambda_x&0&0\\0&\Lambda_y&0\\0&0&\Lambda_z\end{bmatrix} \ , \tag{B10a}$$

$$\langle Q(\mathbf{q}_0)\rangle=\frac{\rho_0}{\sqrt{2}}e^{i\varphi} \ . \tag{B10b}$$

Equations (B7)–(B9) make clear that the excitations at $-\mathbf{q}_0+\mathbf{K}$ and $\mathbf{q}_0+\mathbf{K}$ are still degenerate, with positive frequencies, but are coupled through $R(\epsilon\mathbf{q}_0-\mathbf{K},\epsilon\mathbf{q}_0+\mathbf{K})$ while, through the third term of Eq. (B7), the acoustic phonons are now coupled to the soft modes. As it is well known, the part of Eq. (B7), which contains only the soft-mode variables may be trivially decoupled through a canonical transformation into amplitudon and phason modes:

$$A(\mathbf{K})=\frac{1}{\sqrt{2}}[Q(\mathbf{q}_0+\mathbf{K})e^{-i\varphi}+Q(-\mathbf{q}_0+\mathbf{K})e^{i\varphi}] \ , \tag{B11a}$$

$$\varphi(\mathbf{K})=\frac{i}{\sqrt{2}}[Q(\mathbf{q}_0+\mathbf{K})e^{-i\varphi}-Q(-\mathbf{q}_0+\mathbf{K})e^{i\varphi}]\ ,$$

yielding

$$\Omega_A^2(\mathbf{K})=2\omega^2(\rho)+\tfrac{1}{2}\sum_{\alpha,\beta}\Lambda_{\alpha\beta}K_\alpha K_\beta\ , \tag{B11b}$$

$$\Omega_\varphi^2(\mathbf{K})=\tfrac{1}{2}\sum_{\alpha,\beta}\Lambda_{\alpha\beta}K_\alpha K_\beta\ . \tag{B11c}$$

Note that because, in the incommensurate phase, $\mathbf{q}_0$ is another reciprocal-lattice vector, we have dropped the index $\mathbf{q}_0$ in Eq. (B11a)–(B11c), writing simply $A(\mathbf{K})$, $\varphi(\mathbf{K})$, $\Omega_A^2(\mathbf{K})$, and $\Omega_\varphi^2(\mathbf{K})$. Furthermore, as stated in Sec. III, the phason and amplitudon have the same damping constant $\Gamma(\mathbf{K})$ that we assume to be smoothly temperature dependent.

Finally, due to the appearance of the +(resp. −) sign in Eq. (B11a) the amplitudon (resp. phason) is essentially even (resp. odd) in the vicinity of $\mathbf{K}=0$. As an elastic strain is an even quantity, one could naively think that, through the third term of Eq. (B7), the acoustic phonon would couple only to the amplitudon. When the $\mathbf{q}$ dependence of Eq. (B9) is properly taken into account, the situation turns out to be more complex, as has been shown, e.g., by Bruce and Cowley,[54] Poulet and Pick,[22] Cowley and Mayer,[24] and briefly discussed in Sec. III: in general the elastic strain also couples to the phason. This term appears when one develops $H^\alpha(-\mathbf{q},\epsilon\mathbf{q}_0+\mathbf{q})$ not in first order in q_α [as we have done in the rhs of Eq. (B9)] but in second order in $q_\alpha q_\gamma$. As this term does not exist when we restrict ourselves to the propagation of the ϵ_3 strain, we shall simply write the contribution of the harmonic couplings to $\Sigma_{\alpha\beta}(\mathbf{q},\omega)$ as:

$$\Sigma_{\alpha\beta}^h(\mathbf{q},\omega)=-\frac{4[(h_{\alpha\alpha}^0-2\epsilon_i^0\delta_{i\alpha}g_{\alpha\alpha})q_\alpha][(h_{\beta\beta}^0-2\epsilon_j^0\delta_{j\beta}g_{\beta\beta})q_\beta]\rho_0^2}{\Omega_A^2(\mathbf{K}=0)-i\omega\Gamma(\mathbf{K}=0)}+\Sigma_{\alpha\beta}^{\mathrm{ph}}(\mathbf{q},\omega) \tag{B12}$$

where $\Sigma_{\alpha\beta}^{\mathrm{ph}}(\mathbf{q},\omega)$ represents the harmonic coupling of the acoustic phonons to the phason. In this expression, we have again supposed $\omega\ll\Omega_A(T)$, $\Gamma(T)$, to be consistent with Eq. (B6).

b. Anharmonic interaction and the self-energy term

As in the high-temperature case, let us consider first that the only relevant part of the self energy (which contributes to the anharmonic term) comes from the first term of Eq. (B2). Even in this simple case, one has to take into account the fact that, in the incommensurate phase, the dynamical variables are no longer $Q(\mathbf{q})$, but $A(\mathbf{K})$ and $\varphi(\mathbf{K})$.

More precisely, let us first consider the case where $\mathbf{q}_1=\mathbf{q}_0+\mathbf{K}$ ($\epsilon=+1$). Inverting Eq. (B11a) yields

$$Q(\epsilon\mathbf{q}_0+\mathbf{K})=\frac{1}{\sqrt{2}}[A(\mathbf{K})-i\epsilon\varphi(\mathbf{K})]e^{i\epsilon\varphi} \tag{B13}$$

so that the replacement of the phonon coordinates by the amplitudon and the phason coordinates transforms Eq. (B2) into

$$i\sum_{\alpha,\mathbf{q},\mathbf{K}}\frac{h_{\alpha\alpha}}{2\sqrt{\rho_m}}(-\mathbf{q},-\mathbf{q}_0-\mathbf{K},\mathbf{q}_0+\mathbf{K}+\mathbf{q})q_\alpha U_\alpha(-\mathbf{q})$$
$$\times[A(-\mathbf{K})+i\varphi(-\mathbf{K})][A(\mathbf{K}+\mathbf{q})-i\varphi(\mathbf{K}+\mathbf{q})]\ . \tag{B14a}$$

Conversely, if one considers the $\epsilon=-1$ case ($\mathbf{q}_1=-\mathbf{q}_0+\mathbf{K}$), Eqs. (B2) and (B13) yield

$$i\sum_{\alpha,\mathbf{q},\mathbf{K}}\frac{h_{\alpha\alpha}}{2\sqrt{\rho_m}}(-\mathbf{q},\mathbf{q}_0-\mathbf{K},-\mathbf{q}_0+\mathbf{K}+\mathbf{q})q_\alpha U_\alpha(-\mathbf{q})$$
$$\times[A(-\mathbf{K})-i\varphi(-\mathbf{K})][A(\mathbf{K}+\mathbf{q})+i\varphi(\mathbf{K}+\mathbf{q})]\ , \tag{B14b}$$

while this second term is *not* related by a $\mathbf{q}_1\Longrightarrow\mathbf{q}_2$ interchange to Eq. (B14a). As, by definition

$$h_{\alpha\alpha}(\mathbf{q},\mathbf{q}_1,\mathbf{q}_2)=h_{\alpha\alpha}(\mathbf{q},\mathbf{q}_2,\mathbf{q}_1) \tag{B15}$$

if, in Eqs. (B14) one neglects the dependence of $h_{\alpha\alpha}$ on $\mathbf{q}$ and $\mathbf{K}$ ($|\mathbf{q}|$ and $|\mathbf{K}+\mathbf{q}|$ being always smaller than $|\mathbf{q}_0|$), the sum of the two terms finally leads to the third-order interaction term

$$\frac{i}{\sqrt{\rho_m}}\sum_{\alpha,\mathbf{q},\mathbf{K}}h_{\alpha\alpha}^0 q_\alpha U_\alpha(-\mathbf{q})[A(-\mathbf{K})A(\mathbf{K}+\mathbf{q})$$
$$+\varphi(-\mathbf{K})\varphi(\mathbf{K}+\mathbf{q})] \tag{B16}$$

the summation being over all the vectors $\mathbf{K}$ in the vicinity of the origin. In analogy with Eq. (B2), Eq. (B16) describes now the simultaneous destruction of an acoustic phonon with vector $\mathbf{q}$, and of an amplitudon (resp. phason) with wave vector $\mathbf{K}$, and the creation of an amplitudon (resp. phason) with wave vector $\mathbf{K}+\mathbf{q}$. There will now be two bubble diagrams, contributing to $\Sigma_{\alpha\beta}^a(\mathbf{q},\omega)$, one for the amplitudon, and one for the phason; they just replace, with the same weight for each of them, the two (identical) soft-mode bubble diagrams corresponding to the two minima at $\epsilon\mathbf{q}_0$.

In fact, as ϵ_i^0 is different from zero below T_I, the elastic strain couples to two soft-mode variables, not only through $h_{\alpha\alpha}^0$, but also through $-2\epsilon_i^0\delta_{i\alpha}g_{\alpha\alpha}$ [cf. Eq. (B9)]. The total contribution of the two bubble diagrams is thus:

$$\Sigma_{\alpha\beta}^a(\mathbf{q},\omega)=-2k_BT[(h_{\alpha\alpha}^0-2\epsilon_i^0\delta_{i\alpha}g_{\alpha\alpha})q_\alpha]$$
$$\times[(h_{\beta\beta}^0-2\epsilon_j^0\delta_{j\beta}g_{\beta\beta})q_\beta]$$
$$\times\sum_{\epsilon=\pm1}\sum_{\mathbf{K}}\frac{1}{\Omega_\epsilon^2(\mathbf{K})\left[\Omega_\epsilon^2(\mathbf{K})-i\omega\dfrac{\Gamma(\mathbf{K})}{2}\right]}\ , \tag{B17}$$

with $\Omega_+^2(\mathbf{K})\equiv\Omega_A^2(\mathbf{K})$; $\Omega_-^2(\mathbf{K})\equiv\Omega_\varphi^2(\mathbf{K})$.

Below T_I, the self energy is the sum of Eqs. (B12) and (B17), while it is given by Eq. (B5) above T_1. When one is interested simply in phonons propagating along $\mathbf{c}^*$, $M_{\alpha\beta}(\mathbf{q},\omega)$ is diagonal in $\alpha\beta$; also for symmetry reasons discussed in Sec. III, there is no coupling between the phason and the longitudinal strain. One can thus extract from $M_{\alpha\beta}(\mathbf{q},\omega)$ a frequency-dependent elastic constant $\tilde{C}_{33}(\omega)$ which may be expressed as

$T > T_I$:

$$\tilde{C}_{33}(\omega)=C_{33}^0-4k_B T h_3^2\frac{1}{(2\pi)^3}\int\frac{d^3K}{\Omega^2(\mathbf{K})\left[\Omega^2(\mathbf{K})-i\frac{\omega}{2}\Gamma(\mathbf{K})\right]} \tag{B18}$$

$T < T_I$:

$$\tilde{C}_{33}(\omega)=C_{33}^0+2g_3\rho_0^2-\frac{4(h_3-2g_3\epsilon_3^0)^2\rho_0^2}{\Omega_A^2(0)-i\omega\Gamma(0)}-2k_B T(h_3-2g_3\epsilon_3^0)^2\frac{1}{(2\pi)^3}\left[\int\frac{d^3K}{\Omega_A^2(\mathbf{K})\left[\Omega_A^2(\mathbf{K})-i\frac{\omega}{2}\Gamma(\mathbf{K})\right]}+\int\frac{d^3K}{\Omega_\varphi^2(\mathbf{K})\left[\Omega_\varphi^2(\mathbf{K})-i\frac{\omega}{2}\Gamma(\mathbf{K})\right]}\right]. \tag{B19}$$

*Permanent address: Institute of Physics, Hanoi, Vietnam.

[1]J. D. Axe, M. Iizumi, and G. Shirane, in *Incommensurate Phases in Dielectrics II,* edited by R. Blinc and A. P. Levanyuk (North Holland, Amsterdam, 1986), p. 1.
[2]D. G. Sannikov and V. A. Golovko, Fiz. Tverd. Tela. (Leningrad) **26**, 1117 (1984) [Sov. Phys. Solid State **26**, 678 (1984)].
[3]M. Iizumi, J. D. Axe, G. Shirane, and K. Shimaoka, Phys. Rev. B **15**, 4392 (1977).
[4]H. Hoshizaki, A. Sawada. Y. Ishibashi, T. Matsuda, and I. Hatta, Jpn. J. Appl. Phys. **19**, L324 (1980).
[5]R. Rehwald, A. Vonlanthen, J. K. Kruger, R. Wallerius, and H. G. Unruh, J. Phys. C **13**, 3823 (1980).
[6]W. Rehwald and A. Vonlanthen, Solid State Commun. **38**, 209 (1981).
[7]V. V. Lemanov, S. Kh. Esayan, and A. Karaev, Fiz. Tverd. Tela. (Leningrad) **28**, 1683 (1986) [Sov. Phys. Solid State **28**, 931 (1986)].
[8]S. Kudo and T. Ikeda, Jpn. J. Appl. Phys. **19**, L45 (1980).
[9]P. A. Fleury, S. Chiang, and K. B. Lyons, Solid State Commun. **31**, 279 (1979).
[10]T. Yagi, M. Cho, and Y. Hidaka, J. Phys. Soc. Jpn. **46**, 1957 (1979).
[11]M. Cho and T. Yagi, J. Phys. Soc. Jpn. **46**, 1957 (1979); **50**, 543 (1981).
[12]G. Hauret and J. P. Benoit, Ferroelectrics **40**, 1 (1982).
[13]Y. Luspin, G. Hauret, A. M. Robinet, and J. P. Benoit, J. Phys. C **17**, 2203 (1984).
[14]J. P. Benoit, G. Hauret, Y. Luspin, A. M. Gillet, and J. Berger, Solid State Commun. **54**, 1095 (1985).
[15]R. Blinc, V. Rutar, B. Topic, F. Milia, and Th. Rasing, Phys. Rev. B **33**, 1721 (1986).
[16]W. Yao, H. Z. Cummins, and R. H. Bruce, Phys. Rev. B **24**, 424 (1981).
[17]L. D. Landau and I. M. Khalatnikov, Akad. Nauk SSR Doklady **96**, 469 (1954).
[18]A. P. Levanyuk, Zh. Eksp. Teor. Fiz. **49**, 1304 (1965) [Sov. Phys. JETP **22**, 901 (1966)].
[19]E. Pytte, Phys. Rev. B **1**, 924 (1970); *Structural Phase Transitions and Soft Modes,* edited by E J. Samuelsen, E. Andersen, and J. Feder (Universitets Forlaget, Oslo, 1971), p. 151.
[20]J. M. Courdille, R. Deroche, and J. Dumas, J. Phys. (Paris) **36**, 891 (1975).
[21]Y. Luspin and G. Hauret, Phys. Status Solidi B **76**, 551 (1976).
[22]H. Poulet and R. M. Pick, J. Phys. C **14**, 2675 (1981).
[23]S. Kh. Esayan and V. V. Lemanov, Izv. Akad. Nauk SSR Ser. Fiz. **47**, 591 (1983).
[24]A. P. Mayer and R. A. Cowley, J. Phys. C **19**, 6131 (1986).
[25]V. A. Golovko and A. P. Levanyuk, Zh. Eksp. Teor. Fiz. **81**, 2296 (1981) [Sov. Phys. JETP **54**, 1217 (1981)].
[26]K. Aiki, K. Hukuda, H. Koga, and T. Kobayashi, J. Phys. Soc. Jpn. **28**, 389 (1970).
[27]A. Lopez Echarri, M. J. Tello, and P. Gill, Solid State Commun. **36**, 1021 (1980).
[28]B. K. Chaudhuri, T. Atake, and H. Chihara, Solid State Commun. **38**, 927 (1981).
[29]I. N. Flerov, L. A. Kot, and A. I. Kriger, Fiz. Tverd. Tela. (Leningrad) **24**, 1673 (1982) [Sov. Phys. Solid State **24**, 954 (1982)].
[30]T. Atake, K. Nomoto, B. K. Chaudhuri, and H. Chihara, J. Chem. Thermodynamics **15**, 383 (1983).
[31]M. Midorikawa, J. Phys. Soc. Jpn. **50**, 2141 (1981).
[32]S. Kudo and T. Ikeda, J. Phys. Soc. Jpn. **50**, 3681 (1981).
[33]S. Shiozaki, A. Sawada, Y. Ishibashi, and Y. Takagi, J. Phys. Soc. Jpn. Lett. **42**, 353 (1977).
[34]M. Quilichini and R. Currat, Solid State Commun. **48**, 1011 (1983).
[35]Sannikov and Golovko, from a related analysis starting from somewhat different experimental data, found $A_0=1.5\times10^{23}$, $B=2.1\times10^{42}$, $h_1,h_2,h_3=-0.31\times10^{26}$, -0.90×10^{26}, 3.6×10^{26}, respectively, and in units of dyn cm^{-2}

$$[C^0]=\begin{bmatrix}5.8\times10^{11} & 1.7\times10^{11} & 1.5\times10^{11}\\ & 5.3\times10^{11} & 2.0\times10^{11}\\ & & 3.8\times10^{11}\end{bmatrix}.$$

Values for the other coefficients listed in our Table I were not determined in their analysis.
[36]B. Topic, U. Haeberlen, and R. Blinc, Phys. Rev. B **40**, 799 (1989).
[37]J. J. L. Horikx, A. F. M. Arts, J. I. Dijkhuis, and H. W. de Wijn, Phys. Rev. B **39**, 5726 (1989).
[38]C. J. de Pater and C. van Dijk, Phys. Rev. B **18**, 1281 (1978).
[39]C. J. de Pater, J. D Axe, and R. Currat, Phys. Rev. B **19**, 4684 (1979).
[40]M. Quilichini (private communication).
[41]C. F. Majkrzak, J. D. Axe, and A. D. Bruce, Phys. Rev. B **22**, 5278 (1980).
[42]H. Mashiyama, J. Phys. Soc. Jpn. **50**, 2665 (1981); S. R. Andrews and H. Mashiyama, J. Phys. C **16**, 4985 (1983).
[43]H.-G. Unruh, W. Eller, and G. Kirf, Phys. Status Solidi A **55**, 173 (1979).
[44]See also, W. K. Lee, H. Z. Cummins, R. M. Pick, and C. Dreyfus, Phys. Rev. B **37**, 6442 (1988).
[45]J. C. Le Guillou and J. Zinn-Justin, Phys. Rev. B **21**, 3976 (1980).
[46]H. Iro and F. Schwabl, Solid State Commun. **46**, 205 (1983); F. Schwabl, J. Stat. Phys. **39**, 719 (1985); F. Schwabl, Ferroelectrics **78**, 215 (1988).
[47]R. Dengler and F. Schwabl, Z. Phys. B **69**, 327 (1987).
[48]B. Luthi and W. Rehwald, in *Structural Phase Transitions I*, edited by K. A. Muller and H. Thomas (Springer-Verlag, Berlin, 1981), p. 131.
[49]J. Hu, J. O. Fossum, C. W. Garland, and P. W. Wallace, Phys. Rev. B **33**, 6331 (1986).
[50]F. Schwabl (private communication).
[51]A. Levanyuk (private communication).
[52]D. G. Sannikov and A. P. Levanyuk, Fiz. Tverd. Tela. (Leningrad) **20**, 1005 (1978) [Sov. Phys. Solid State **20**, 580 (1978)]; V. Dvorak and O. Hudak, Ferroelectrics **46**, 19 (1982); Y. Ishibashi, in *Incommensurate Phases in Dielectrics II*, edited by R. Blinc and A. P. Levanyuk (North Holland, Amsterdam, 1986), p. 49.
[53]V. L. Ginzburg, A. P. Levanyuk, and A. A. Sobyanin, Phys. Rep. **57**, 151 (1980).
[54]A. D. Bruce and R. A. Cowley, J. Phys. C **11**, 3609 (1978).